

Electrocorticographic Analysis of Spontaneous Conversation
to Localize Receptive and Expressive Language Areas

by

Jennapher Lingo VanGilder

A Thesis Presented in Partial Fulfillment
of the Requirements for the Degree
Master of Science

Approved July 2013 by the
Graduate Supervisory Committee:

Stephen Helms Tillery, Co-Chair
Remy Wahnoun, Co-Chair
Christopher Buneo

ARIZONA STATE UNIVERSITY

AUGUST 2013

ABSTRACT

When surgical resection becomes necessary to alleviate a patient's epileptiform activity, that patient is monitored by video synchronized with electrocorticography (ECoG) to determine the type and location of seizure focus. This provides a unique opportunity for researchers to gather neurophysiological data with high temporal and spatial resolution; these data are assessed prior to surgical resection to ensure the preservation of the patient's quality of life, e.g. avoid the removal of brain tissue required for speech processing. Currently considered the "gold standard" for the mapping of cortex, electrical cortical stimulation (ECS) involves the systematic activation of pairs of electrodes to localize functionally specific brain regions. This method has distinct limitations, which often includes pain experienced by the patient. Even in the best cases, the technique suffers from subjective assessments on the parts of both patients and physicians, and high inter- and intra-observer variability. Recent advances have been made as researchers have reported the localization of language areas through several signal processing methodologies, all necessitating patient participation in a controlled experiment. The development of a quantification tool to localize speech areas in which a patient is engaged in an unconstrained interpersonal conversation would eliminate the dependence of biased patient and reviewer input, as well as unnecessary discomfort to the patient.

Post-hoc ECoG data were gathered from five patients with intractable epilepsy while each was engaged in a conversation with family members or clinicians. After the data were separated into different speech conditions, the power of each was compared to

baseline to determine statistically significant activated electrodes. The results of several analytical methods are presented here.

The algorithms did not yield language-specific areas exclusively, as broad activation of statistically significant electrodes was apparent across cortical areas. For one patient, 15 adjacent contacts along superior temporal gyrus (STG) and posterior part of the temporal lobe were determined language-significant through a controlled experiment. The task involved a patient lying in bed listening to repeated words, and yielded statistically significant activations that aligned with those of clinical evaluation. The results of this study do not support the hypothesis that unconstrained conversation may be used to localize areas required for receptive and productive speech, yet suggests a simple listening task may be an adequate alternative to direct cortical stimulation.

ACKNOWLEDGEMENTS

This study would not have been possible without the joint collaboration of Barrow National Institute at Phoenix Children's Hospital and the Mayo Clinic with Arizona State University. Specifically, the mentorship of Dr. Remy Wahnoun and Dr. Stephen Helms Tillery were crucial to the consummation of this study.

Funding was provided by an Arizona Biomedical Research Commission grant, "A Practical Brain-Computer Interface" awarded to Dr. Stephen Helms Tillery and Dr. David Adelson.

TABLE OF CONTENTS

	Page
LIST OF TABLES.....	vi
LIST OF FIGURES.....	vii
INTRODUCTION.....	1
REVIEW OF LITERATURE.....	4
STATEMENT OF THE PROBLEM.....	11
HYPOTHESIS.....	11
MATERIALS AND METHODS.....	12
Subjects.....	12
Direct Cortical Stimulation.....	13
ECoG Data.....	14
Estimation of Power.....	15
Statistical Analyses.....	17
RESULTS.....	20
DISCUSSION.....	21
Conclusions.....	22
Limitations.....	23
Future Work.....	24
REFERENCES.....	26
APPENDIX	
I BRAIN SKETCHES OF SIGNIFICANT ACTIVATIONS.....	30

II INSTITUTIONAL REVIEW BOARD APPROVAL FORM..... 60

LIST OF TABLES

Table	Page
1. Patient Demographics.....	12
2. Patient Speech Contacts.....	13

LIST OF FIGURES

Figure	Page
1. ECoG Data Processing.....	17
2. Methods Flowchart: Continuous Conversation Stream	19
3. Methods Flowchart: Individual Speech Conditions.....	19
4. Patient 1 Brain Sketch Segments.....	20
5. Patient 5 Brain Sketch Speaking.....	21
6. Patient 1 Brain Sketch Segments.....	31
7. Patient 1 Brain Sketch Segments (Frequency Ranges).....	32
8. Patient 1 Brain Sketch Ratios.....	33
9. Patient 1 Brain Sketch Ratios (Frequency Ranges).....	34
10. Patient 1 Brain Sketch Combined Speech (Segments).....	35
11. Patient 1 Brain Sketch Combined Speech (Ratios).....	36
12. Patient 2 Brain Sketch Segments.....	37
13. Patient 2 Brain Sketch Segments (Frequency Ranges).....	38
14. Patient 2 Brain Sketch Ratios.....	39
15. Patient 2 Brain Sketch Ratios (Frequency Ranges).....	40
16. Patient 2 Brain Sketch Combined Speech (Segments)	41
17. Patient 2 Brain Sketch Combined Speech (Ratios)	42
18. Patient 3 Brain Sketch Segments.....	43
19. Patient 3 Brain Sketch Segments (Frequency Ranges).....	44
20. Patient 3 Brain Sketch Ratios.....	45

Figure	Page
21. Patient 3 Brain Sketch Ratios (Frequency Ranges).....	46
22. Patient 3 Brain Sketch Combined Speech (Segments).....	47
23. Patient 3 Brain Sketch Combined Speech (Ratios).....	48
24. Patient 4 Brain Sketch Segments.....	49
25. Patient 4 Brain Sketch Segments (Frequency Ranges).....	50
26. Patient 4 Brain Sketch Ratios.....	51
27. Patient 4 Brain Sketch Ratios (Frequency Ranges).....	52
28. Patient 4 Brain Sketch Combined Speech (Segments)	53
29. Patient 4 Brain Sketch Combined Speech (Ratios)	54
30. Patient 5 Brain Sketch Listening Activations.....	55
31. Patient 5 Brain Sketch Speaking Activations.....	56
32. Patient 5 Brain Sketch Listening to Words Activations.....	57
33. Patient 5 Brain Sketch Reading Activations.....	58
34. Patient 5 Brain Sketch Speech Combined Activations.....	59

INTRODUCTION

It is estimated that 2.5 million Americans are afflicted with epilepsy, and 65 million people worldwide. Nearly a tenth of the population will have at least one seizure during their lifetime (W.H.O. 2012, Epilepsy Foundation 2012). Seizures are episodes of abnormal electrical activity of the brain which can arise from multiple brain foci or from a single, localized focus. These electrical discharges can disrupt normal function (clinical seizure) or remain undetected by the patient (electrographic seizure). During a clinical seizure (seizure that exhibits clinical symptoms), one may experience unconsciousness, involuntary muscle contractions, postictal confusion, and memory loss (Schachter 2006), diminishing one's quality of life.

When the administration of antiepileptic drugs (AEDs) is ineffective in treating seizure formation, a patient may qualify for a more aggressive treatment modality. In some cases surgery involving the removal of afflicted brain tissue can alleviate epileptic symptoms. Individualized consideration is taken to evaluate each patient's candidacy for resection surgery; continued seizures and high doses of medication may affect a person's emotional, psychological, social, or professional life (Weiner 2004), and are weighed against the risks involved with surgery.

To assess one's candidacy for surgical resection, it's essential to first analyze the epileptiform signals, including their origin and propagation. In many hospitals, this electrical activity is assessed by monitoring the patient via videotape synced with encephalography (EEG) in the Epilepsy Monitoring Unit (EMU). If it appears the seizures originate in or near critical brain structures that could result in long-term functional deficits, e.g. language areas, or somatosensory and motor cortices, or the

seizures are general in nature, surgical resection is not an option (Hill *et al.* 2012). Patients identified as potential candidates for resection will undergo a preliminary surgery involving the implantation of an electrocorticographic (ECoG) grid(s). This grid is placed on the surface of the patient's brain at the surgeon's discretion, and is used to more accurately depict the location of seizure focus and the function of adjacent cortical structures. The patient will again be closely monitored via videotape synced with ECoG. Cortical mapping of regions required for higher-order cognitive processes is crucial to ensure functionality is preserved during surgical resection as well as to further the current understanding of integrated brain processes. Pairs of electrodes are systematically activated to identify brain areas that elicit motor responses or inhibit language function, with the aim of generating a cortical topographical map. After a pair of electrodes is stimulated the patient is asked to describe the sensation; this method heavily relies on the accuracy and clarity of the patient's response. Although currently considered the "gold standard" for mapping cortex, cortical stimulation is imperfect, inconvenient, at times extremely painful, and patients often experience seizure onset when the focus is localized. Additionally, the inaccuracy and inconsistencies of EEG reporting has become the subject of discussion among researchers, specifically the lack of standardized protocol and nomenclature used throughout analysis (Benbadis *et al.* 2009, Gerber *et al.* 2008, Haut *et al.* 2002, Wu *et al.* 2010). In fact, a large number of patients will continue to have seizures after treatment (Sun *et al.* 2007), possibly due to the imprecision of source localization. The use of quantitative tools to assess these data would help eliminate the inaccuracy of subjective patient and reviewer input, and therefore reduce the existence of

inter- and intra-observer variability between reviewers (Lodder and J.A.M. van Putten 2013).

The higher-level processing involved in the ability to interpret and express verbal communication is central to one's daily life, yet its functional organization remains uncertain. It is known that language areas vary broadly among patients, further highlighting the necessity of identifying these areas before resection. The implantation of ECoG grids provides a unique opportunity for epileptologists to record and stimulate areas of the brain as well as for researchers to gather neurophysiological data containing high temporal and spatial resolution; these data may be key in the development of an automated quantification tool to localize language areas, which would avoid dependence on subjective patient and reviewer input as well as unnecessary inconveniences to the patient. As such, the purpose of this research is to determine the plausibility of developing an algorithm to successfully identify receptive and expressive speech areas of post-hoc ECoG data, specifically in which the patient was engaged in an uncontrolled interpersonal conversation.

REVIEW OF LITERATURE

The first language center was identified in 1861 by the French neurosurgeon, Paul Broca. Broca worked closely with patients who could comprehend language, yet were unable to express themselves verbally nor in writing. His famous patient “Tan”, was nicknamed so because after suffering a traumatic brain injury (TBI), it was the only word he could stutter. After Tan’s death, Broca performed an autopsy and discovered a lesion across the lateral surface of the left frontal lobe (Dronkers *et al.* 2007). Through comparison with subsequent patients with similar disability, Broca confirmed the posterior-inferior frontal gyrus of the left cerebral hemisphere as an important area for speech production, and it was dubbed “Broca’s area” accordingly. “Broca’s aphasia” was coined in reference to any deficit in language articulation, thus implicating all aspects of the disorder to this one brain region.

Similarly, Karl Wernicke studied aphasic patients to localize areas that correlate to speech perception. However, Wernicke’s patients were unable to interpret written or spoken words, resulting in the production of meaningless speech despite maintaining the ability to physically articulate language (McCaffey 2008). His patients had lesions on the posterior region of the superior temporal lobe (STG) of the left hemisphere and he identified this as “area of word images” (Weisman *et al.* 2003), further confirming Broca’s hypothesis of the left hemisphere as significant for language function. Wernicke also realized the importance of the arcuate fasciculus (AF) in the transfer of information between the anterior and posterior language centers and posited that damage to this structure would result in a ‘fluent speech disorder with good comprehension, yet with

impaired spontaneous speech, naming, and repetition' (Anderson *et al.* 1999). As in the case of Broca, "Wernicke's aphasia" and "conduction aphasia" were used in reference to specific deficits in speech perception.

Although Wernicke's and Broca's work laid the foundation for the modern understanding of language processing, advancements in neuroimaging techniques have improved our general understanding of neural processes. Recent studies have challenged the traditional conceptualization of these brain regions being solely responsible for speech expression and perception. Dronkers *et al.* retrieved the preserved brains of Broca's patients, assessed the extent of their conditions via magnetic resonance imaging (MRI), and reported that each had significant medial lesions in addition to the lateral surface lesions- signifying that the posterior-inferior frontal gyrus does not singularly contribute to language production. Further, Fridriksson *et al.* (2007) employed several neuroimaging methods to present a case study involving a patient that suffered a subcortical hemorrhagic stroke, inducing severe Broca's aphasia. Assessing the patient's functional MRI (fMRI), it was evident the patient did not sustain Broca's area damage; however further analysis through the use of tractology revealed a clear disconnect between Broca's and Wernicke's areas, via arcuate fasciculus. Wernicke's postulate has also been challenged, specifically the role of the AF in conduction aphasia. Researchers have repeatedly shown through a variety of neuro- anatomical and -physiological techniques that cortical dysfunction alone may result in this disorder (Anderson *et al.* 1999, Bernal and Ardila 2009, Selnes *et al.* 2010, Hyeok and Sung 2011).

Over the past 150 years researchers have studied language processing to establish that language function is the result of a complex network of multiple cortices. The most widely accepted model involves localized brain areas that encode for specific functions as well as “participate in networks employing multiple brain regions” required for higher-order processing (Blumenfeld 2002, p. 827). Wernicke’s area has been more clearly defined to Brodmann’s area 22, or the posterior two-thirds of the STG of the dominant hemisphere; Blumenfeld states other authors often include Brodmann’s areas 37, 39, and 40 within Wernicke’s area as damage to these areas cause Wernicke’s aphasia. Broca’s area corresponds to Brodmann’s areas 44 and 45, and rests in the inferior frontal gyrus; some authors include the adjacent areas 9, 46, and 47 while others go even further to include areas 6, 8, and 10 as damage to these areas can cause Broca’s aphasia (Blumenfeld 2002, p. 829).

Although Broca’s and Wernicke’s areas are critical for language production and comprehension, both regions depend on reciprocal connections with surrounding cortex for higher-order functioning (Blumenfeld 2002, p. 829). The anterior regions of Broca’s area are key for correct syntax in expressive and receptive speech, while the premotor cortex functions as an aid in speech planning and formulation (Duffau *et al.* 2003).

Similarly, the cortex immediately posterior to Wernicke’s area contains the lexicon, used in both speaking and listening, while the angular gyrus is central to one’s ability to read. Wise *et al.* (2001) examined several positron emission tomography (PET) studies to localize functionally specific and anatomically separate streams of auditory processing found posterior to the auditory cortex; their findings include areas of activation

correlating to speech production at the junction of the inferior parietal lobe and posterior temporal lobe. Blumenfeld states the connections through the corpus callosum allow the non-dominant hemisphere to contribute a deeper understanding of affective elements in speech (Blumenfeld 2002, p. 829). Additionally, recent evidence has shown frontal lobe “corollary discharges” suppress the activity of receptive areas in the temporal lobe while speaking (Towle *et al.* 2008), which is hypothesized to explain the low level of attention given to one’s voice.

The complexity of language’s intertwined neuronal networks is further emphasized as numerous studies report the significance of the motor system during both speech articulation and comprehension. Hanlon *et al.* (1990) evaluated a variety of patients with differing aphasic subtypes and report gestures that activate the right-shoulder musculature enhances the naming performance of Broca’s aphasic subjects exclusively. They postulate that during communicative gestures, functional activation of the primitive motor system allows access to the initial formative process, and climactically results in speech production. These findings suggest sophisticated language processing evolved from and is significantly influenced by motor system recruitment. As an extension of this work, Topper *et al.* (1998) applied focal transcranial magnetic stimulation (TMS) to the motor cortex for proximal arm muscles and to Wernicke’s cortex in non-aphasic subjects. Contributing to the postulate that motor programming and language processing have overlapping neuronal networks, and that perisylvian stimulation will preactivate the receptive language network, Topper *et al.* conclude TMS over Wernicke’s area facilitates a significant decrease in picture-naming latencies. Other researchers’ findings align with

this paradigm in which anterior vs. posterior localizations for language function are interconnected and interdependent for the generation of receptive and expressive speech (Towle *et al.* 2008, Edwards *et al.* 2010, Wise *et al.* 2001, Lieberman *et al.* 1967, Wilson *et al.* 2004).

Given the complexity of the language network, it is imperative to wholly identify language areas before surgical resection. Currently considered the best method to map cortex, cortical stimulation involves the electrical stimulation between pairs of electrodes in attempt to localize the function of specific brain regions. Cortical stimulation relies on the patient's ability to participate and effectively communicate a sensation, which is not always optimal in patients who are being treated with heavy doses of peri-operative analgesics, or especially in young children. Furthermore, the accuracy in which these tests are reported has been drawn into question. Many researchers have shown high inter-rater variability within the reports among different reviewers and state standardized protocol, especially terminology, is clearly needed for the assessment of EEG reports (Haut *et al.* 2002, Benbadis *et al.* 2009, Gerber *et al.* 2008). Though the instantiation of a standard guideline would improve the efficiency and possibly accuracy of these reports, an automated quantification tool for the localization of language areas would eliminate these issues all together.

Several researchers have paved the road for speech localization through EEG and ECoG analysis in controlled experiments. Though neither recording modalities are considered the "gold standard" for determining eloquent cortex (Towle *et al.* 2008), both exhibit long-term stability in signal acquisition as they avoid brain penetration. While EEG is

non-invasive, ECoG has several advantages over EEG. Unlike EEG, ECoG grids are subdural, have the ability to record at frequencies greater than 70 Hz (high gamma frequencies), and have enhanced spatial resolution and signal magnitude (Leuthardt *et al.* 2011). Leuthardt *et al.* state these higher frequencies are associated with speech functions in humans as well as being central to BCI operation. For these reasons, researchers prefer electrocorticography as a recording modality when studying task-related spectral modulations as it provides robust neural data whereas EEG lacks general recording quality.

Functional activation of eloquent cortex is associated with event- or task-related signals in the high-gamma band (Sinai *et al.* 2005, Ray *et al.* 2008, Ball *et al.* 2008, Wu *et al.* 2010). These high frequencies contain an increase in spectral amplitude affiliated with numerous motor, language, and cognitive tasks (Crone *et al.* 2001, Crone *et al.* 1998, Leuthardt *et al.* 2007). Though specific cutoff frequencies vary from study to study, the findings align to report an increase in high gamma activity over localized areas during language tasks. Towle *et al.* considered the frequencies 70 Hz to 100 Hz and report perisylvian frontal, parietal, and temporal cortical areas demonstrate localized high-frequency gamma activity during listening, interpreting, and speech articulation.

Interestingly, they report electrodes along the temporal lobe show selective activation while hearing and repeating words, as whereas electrodes in the premotor hand area can be activated while listening. Cho-Hisamoto *et al.* (2012) recorded data from a spontaneously cooing and babbling infant and found significant gamma-augmentation (30 Hz to 100 Hz) in the STG and Rolandic areas. Others have assessed a broader range

of high gamma (70 Hz to 170 Hz, 200 Hz) frequencies for the partial decoding of speech (Kellis *et al.* 2010, Pei *et al.* 2011).

Though these studies clearly indicate the actuality of mapping receptive and expressive language areas without ECS, they require the participation of distressed patients in controlled experiments. The results of a recent study suggest the importance of spontaneous conversations to fully localize language areas. Cervenka *et al.* (2013) have shown that subjects who name an object when presented with an auditory descriptive phrase exhibit activations in high gamma frequencies over language areas not present during the visual presentation of the object. These locations were not identified during ECS, which highlights a substantial limitation of cortical stimulation in language mapping, but more importantly provides evidence that the use of unconstrained conversations to wholly identify speech areas is crucial, as conversing requires syntactic and phonetic processing. Further, although they have not yet shown these results, Towle *et al.* have hinted at the plausibility of using post-hoc ECoG data of patient conversations to identify expressive and receptive speech areas.

STATEMENT OF THE PROBLEM

The most commonly used method to identify language areas involves direct cortical stimulation which requires patient participation and is often noxious as well as inconsistent. Previous studies have demonstrated the actuality of localizing speech areas during controlled language tasks, yet none have presented scientific evaluation of spontaneous speech. Developing an automated algorithm that identifies these areas through post-hoc ECoG data would eliminate unnecessary inconveniences to the patient and could provide another benchmark to reduce misinterpretation issues by reviewers.

HYPOTHESIS

ECoG data containing spontaneous conversations can be used to develop an automated algorithm that localizes expressive and receptive language areas for surgical planning. I expect to find activations associated with task-related augmented power (between the frequencies of 70 Hz and 110 Hz) over Wernicke's area, throughout the STG, and possibly in premotor hand area (Towle et al. 2008) when the patient is perceiving speech. Additionally, I expect to find statistically significant activations over Broca's area and its surrounding cortex, and possibly throughout the frontal lobe during productive speech (Blumenfeld 2002, p.827). Although patient cortical stimulation reports are sometimes misleading and not wholly representative of language areas, I anticipate an alignment between statistically-significant activated electrodes with those found clinically.

MATERIALS AND METHODS

All procedures were approved by the Institutional Review Board of Phoenix Children’s Hospital and the Mayo Clinic; the approval form can be viewed in Appendix II.

Subjects

Post-hoc ECoG data were extracted from five patients with intractable epilepsy. Patient demographics, grid placement, and ictal contacts are shown in Table 1 below.

Table 1. Patient Demographics

Patient	Age	Gender	R/L Hand Dominant	Grid	Ictal Contacts
1	21	F	R	LT LIF LSF LPF LPT LAT	LIF2 5 LSF3 LPF4 LT5 12 17 LAT5 6
2	62	M	Unknown	G S	G1 9 20
3	34	F	Unknown	RFG RTG LT	RTG 5 10 15
3	66	M	R	G1 G3 D1 D3	G3.1-5
4	15	M	R	OS TS G LIH	G7 G8 G15 G16 G39 G40 G47 G48 G55 G56

Table 1: Patient demographics and seizure information. LT-left temporal, LIF-left inferior frontal, LSF-left superior frontal, LPF-left posterior frontal, LPT-left posterior temporal (depth), LAT-left anterior temporal (depth), G-temporal gyrus, S- posterior temporal gyrus, OS- occipital, LIH- left hemispheric, TS- temporal superior, G- posterior auditory cortex-occipito-parietal, RGF- right frontal, and RTG- right temporal.

Throughout the duration of each patient’s visit, antiepileptic drugs (AEDs) were tapered to induce the presence of seizures. Data were extracted during stable interictal periods after seizures had been identified by epileptologists via ECoG video monitoring. The grids (Ad-Tech) were platinum silicon arrays with a contact diameter of 1 mm and spacing of 1 cm. The amount and type of array(s) were determined by the clinical needs of the patient. Four of the five patients received implantations to the left hemisphere, varying in number and location, while one patient was implanted on the right hemisphere. Grid location relative to anatomical gyri was estimated by cross-referencing the patient’s

EEG report with the coronal and sagittal views of their computed tomography (CT) images.

Direct Cortical Stimulation

Electrical cortical stimulation for four of the five patients was conducted at bedside with the patient in supine position. Stimulation was performed per standard protocol using a Grass stimulator with gradually increasing stimulation delivered to select electrodes; pairs of electrodes were systematically stimulated to identify eloquent cortex. After each individual discharge, patients were asked to report signs or symptoms in an attempt to localize functionally specific brain regions; depending on the location of the array, behavioral and/or linguistic tasks were utilized.

One patient did not receive ECS, and language areas were clinically determined by fMRI.

Findings from direct cortical stimulation reports for all patients are listed in Table 2 below. Notice a few patients have unspecified language and motor tasks as well as grids positioned solely in suspected receptive speech areas.

Table 2. Patient Speech Contacts

Patient	DCS test	Speech Contacts (Clinical)
1	Reading	LT15 LT19 LT20
2	Unspecified language	G19 G20 S5 S6 (Possibly S3 S4)
3	None (fMRI-reading)	Unknown-bilateral
4	Motor tasks	G3.13 G3.18
5	Listened to repeated words	G41 42 43 44 49 50 51 57 58 59 60 TS3 4 5 6

Table 2: Language-significant electrodes found clinically for each patient.

EECoG Data

EECoG data synced with video were recorded continuously at 500 Hz (XL-tech Ltd., EMU128 amplifier) for the duration of the patient's visit. In the interest of conserving space on the hospital's server, much of the patient data had been deleted by EEG technicians prior to this post-hoc study. This left a total of five patients with ideal grid placement and sufficient data to complete this study. The data were identified during stable interictal periods, in which each patient was engaged in conversation with family members or clinicians. To separate the data into different speech conditions, patient videos were assessed to record the start and end time of each language segment. All patients contained segregated speaking, listening, and baseline segments. For two of the five patients reading data were also available. Due to the limited availability of data in this study, baseline was considered as an instance in which no one was performing a speech function, though some patients had background noise including television or music. As the study evolved, the data analysis approach changed several times resulting in different extraction methods. As such, four of the five patients' data are entire conversations and were extracted from data at the Mayo Clinic, while the fifth patient's data were taken from Phoenix Children's Hospital and each file is comprised of individual speech segments.

All data manipulation was performed in Matlab software (MathWorks 2012). Data were extracted in a European Data Format (EDF), which is used for the exchange and storage of medical physiological data; the files were then converted into a readable Matlab format using a custom-written Matlab program.

Estimation of Power

As this study attempts to determine the plausibility of utilizing spontaneous conversation to fully localize speech areas, a variety of signal processing modalities were employed. All calculations for every patient were performed after the removal of dead channels as well as those known to contain seizure activity and obvious external noise.

For four of the patients, power was estimated for each individual condition using the Hilbert Transform (HT) at the median frequencies of the high gamma range (84.96 Hz and 142.5 Hz) (Towle *et al.* 2008) as well as averaged across the high gamma band (70 Hz-110 Hz and 130 Hz -170 Hz). The HT estimates instantaneous power, i.e. it yields accurate power across time-series data - which is useful when segmenting each speech condition across the continuous conversation stream. Since all of Patient 5's speech conditions are in separate files, power was estimated via spectrogram at the same frequencies (specified above). When power is estimated using a spectrogram, the data lose time information of the signal; this is because it utilizes a fast Fourier transform (FFT) which transforms data from the time domain to the frequency domain. All power estimations avoided the line noise evident at: 60 Hz, 120 Hz, 180 Hz, and 240 Hz, and were used in each of the analysis methods described below.

For each of the four patients, all similar speech segments (speaking, listening, baseline, etc.) were first combined and compared to baseline. Statistical data analysis was then performed to assess the significance of each electrode for each speech condition. The second method combined all similar speech segments and divided by the average power of baseline to generate power ratios. This was used to clearly distinguish an

augmentation in task-related power (value greater than 1 indicates power increase).

Baseline was normalized and then compared to receptive and expressive speech power ratios in a statistical test for significance. The last method combined all speech segments together (power was estimated at 84.96 Hz and 142.5 Hz) and then compared to baseline (Towle *et al.* 2008).

A second set of data were generated by performing independent component analysis (ICA) for each of the four patients. This de-noising method is a blind source separation (BSS) which allows the removal of statistically independent signal components. Both power estimations were performed and run through the three different techniques with this data.

The last patient (P5) contained data in which each speech segment had been extracted as an individual file; therefore the time-series data are insignificant during analysis, and the power of each speech condition was estimated via spectrogram that averaged frequency ranges from 70 Hz to 110 Hz and 130 Hz to 170 Hz. This was also the only patient to contain a grid of 64 electrodes, which has been cited as the minimum number to allow a common-average reference (CAR) (Dien 1998). Several language conditions were available for P5, including reading, listening to words (with eyes closed), speaking, baseline, and listening during a conversation. The segments were compared to baseline and tested for statistical significance. Lastly, all speech conditions were combined (Towle *et al.* 2008) and compared to baseline.

Statistical Analyses

The data were assessed by the Wilcoxon rank-sum statistical test to account for the data's non-parametric attributes. This is a two-sample t-test that is based on the order of which baseline and each specific language segment falls. Each test was calculated with an alpha value of 0.05 to determine the statistical significance with 95% confidence.

To clarify the analytic process, the following figures are presented. Figure 1 illustrates the separation of speech data.

Figure 1. ECoG Data Processing

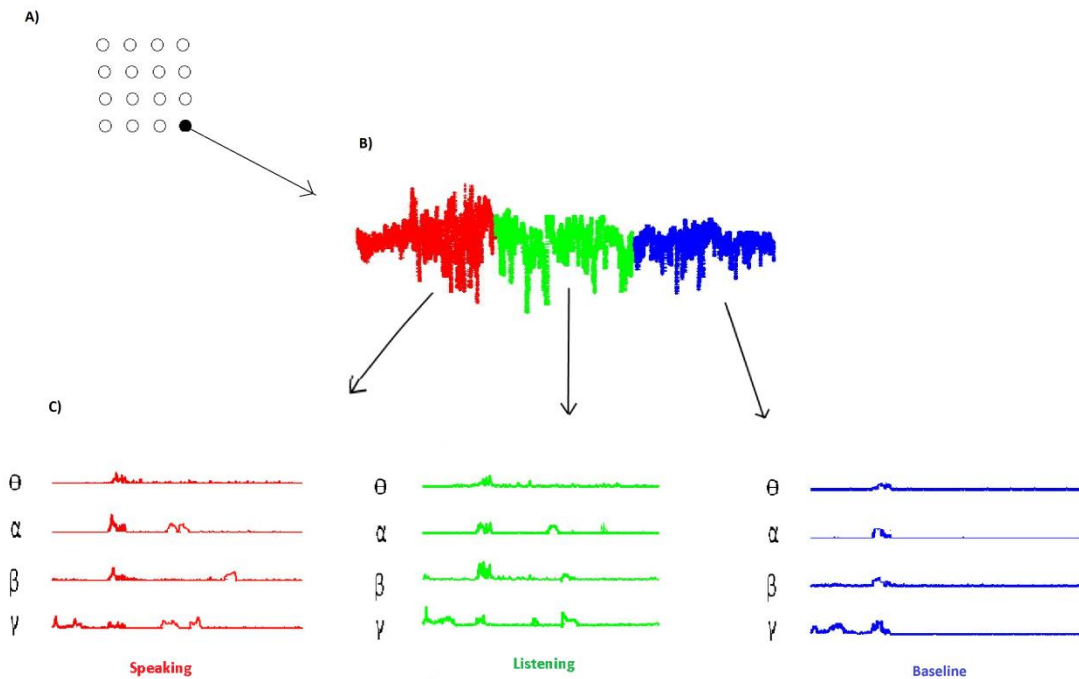
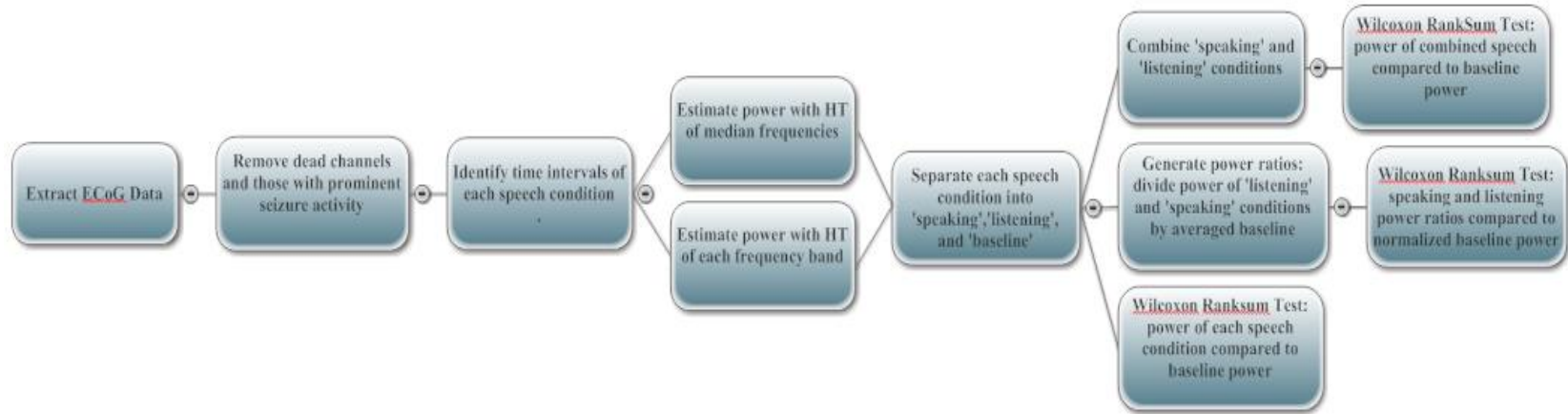


Figure 1: Illustration of ECoG signal analysis: A) 4x4 ECoG grid; B) Raw signal with separate colors representing different speech conditions; C) Speaking, listening, and baseline power plots for each frequency band (Theta 4-8 Hz; Alpha 8-14 Hz; Beta 14-30 Hz; Gamma 30-250 Hz).

After the power of each speech condition is estimated (seen in Fig.1 (C)), one of several analytic methods are employed and then statistically tested. Figures 2 and 3 illustrate the sequence of steps taken throughout the analytic process. Figure 2 presents the methods for the first four patients (continuous conversation stream data). Patient 5's data did not require segregation into similar speech conditions (as the extraction process separated them), and therefore had a slightly different processing method than the first four patients; this is presented in Fig. 3.

Figure 2. Methods Flowchart: Continuous Conversation Stream



19

Figure 2: Flowchart explaining the sequence of steps taken during analysis for Patients 1-4.

Figure 3. Methods Flowchart: Individual Speech Conditions

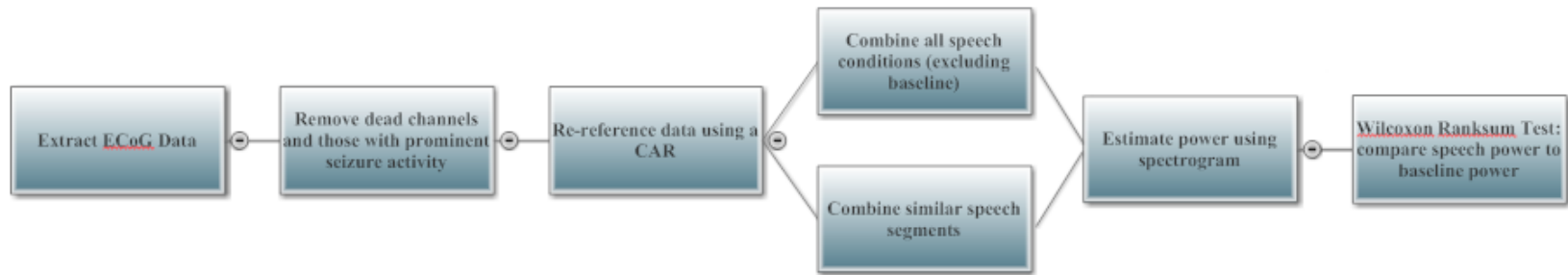


Figure 3: Flowchart explaining sequence of steps taken during analysis of Patient 5.

RESULTS

All patient brain sketches containing electrodes in which each language activity was significantly different from baseline for each calculation method are located in Appendix I; each has a caption noting any interesting characteristics- please refer to them as needed. Only two figures are presented in this section as they are representative of the results across all patients.

Figure 4: Patient 1 Brain Sketch Segments

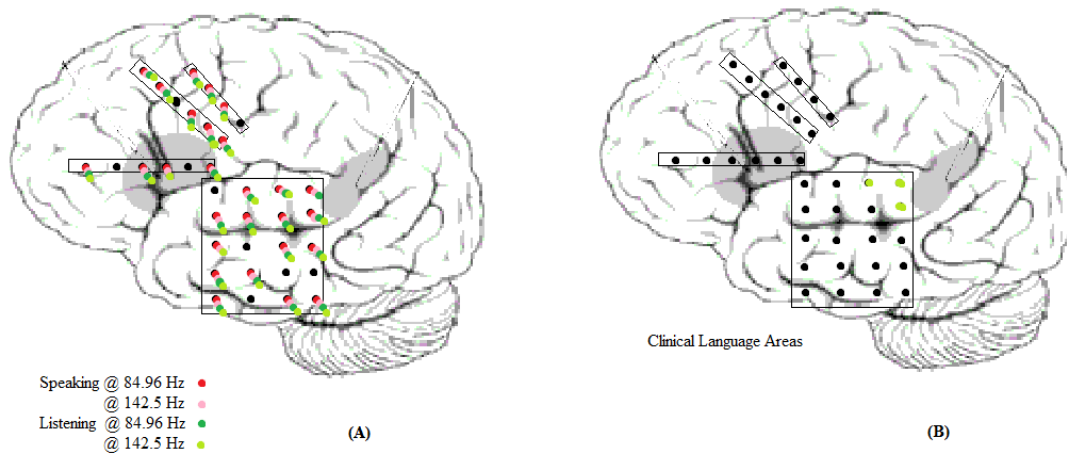


Figure 4: Two brains with electrodes found to be language-specific. Brain (A) illustrates widespread statistically significant electrode activations during both listening and speaking conditions for Patient 1. The power of each language condition was estimated by the HT from the above frequencies and separated into similar segments; speaking and listening were then compared to baseline. The black electrodes were removed from analysis (dead channel or contained prominent seizure activity). Again, grid locations are estimated from cross-referencing CT images with patient reports.

Notice every contact was activated for both conditions except listening at 84.96 Hz in suspected Broca's area and primary auditory cortex, and listening at 142.5 Hz near Wernicke's area.

Figure 5: Patient 5 Brain Sketch Speaking

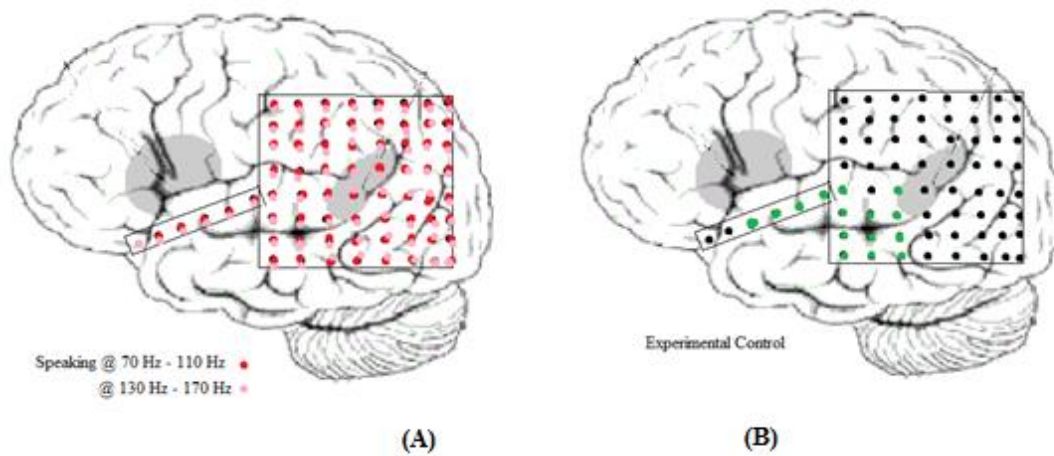


Figure 5: Two brains from Patient 5 with language-specific electrodes. Brain (A) illustrates activations found while the patient was speaking during an unconstrained conversation. Brain (B) shows significant activations during an experiment in which the patient was listening to a computer generate words. Power was calculated by a spectrogram.

Notice every electrode was significantly different than baseline during this speech condition.

DISCUSSION

The success of this study is not measured by the alignment of contacts found by each method and of those determined clinically. Little comparison was made between my results and the DCS reports as they are not wholly representative of language areas and are, at times, inaccurate. Further, analysis in this study is qualitative as grid placement is inferred and true language areas are unknown.

All patient brain sketches contain broad activations across cortex during each speech condition. These could represent functional activations due to distractions (e.g. occipital and motor area recruitment), and may be an indicator that spontaneous conversation is too unconstrained to localize speech-specific regions.

Conclusions

The study doesn't yield results which lead to clear, distinct results, yet I draw several conclusions nonetheless.

Most importantly, my data do not support the hypothesis that spontaneous conversations can be used to localize receptive and expressive language areas. However, this study suffers some key limitations. First, the data sets lack adequate baseline data needed for comparison. All speech conditions were tested for statistical significance against baseline, so an insufficient sample would yield inaccurate results.

Also, since language function is the result of interconnected neuronal networks, it's likely that functional activation occurs across many high frequencies. Though using the specific frequencies of 84.96 Hz and 142.5 Hz was adequate for Towle *et al.*'s study, this method is not advised for future investigations. The latter ignores all high-gamma frequencies other than those specified, which can exclude important features. For example, in this study P5's receptive areas were found at 93 Hz during the experimental control. Data analysis should include a range of frequencies across the high gamma spectrum.

A last thought on the pursuit of spontaneous conversation analysis: in consideration of the two data extraction methods, extracting conversation data as a continuous stream may yield better results. In this way any underlying artifacts or signal noise would be uniform across language conditions. This would be more accurate than making the contrast between a baseline and speaking segment recorded in different environments.

It is important to keep in mind the goal of this research: localize speech areas as non-invasively as possible. Though a simple reading or listening task requires patient participation, it may be an adequate substitution for cortical stimulation. Along that line of thought, the controlled experiment for P5 is the most non-invasive, as it involved the patient lying in bed, listening to a computer repeat words.

Limitations

There are several distinct limitations to this study. The most obvious is the estimation of electrode locations due to insufficient patient radiological records. Patient MRI and CT DICOMs would yield precise electrode positions, therefore enabling further quantitative analysis (McAndrew *et al.* 2011). Additionally, the number and location of the grids are placed at the surgeon's discretion, often limiting analysis to a small area.

Another complication is data quality. All data were taken from epileptic patients in which electrographic seizures could mistakenly be considered task-related activations. Further, the amount of data was limited - few patients had desired grid placement as well as sufficient conversation data. This often necessitated extracting data segments from conversations during meals, which can enhance the presence of artifacts.

Finally, using ECoG data from spontaneous conversations has suffers from a lack of behavioral control. For instance, a patient's attention cannot be accounted for during each speech condition, especially while listening (e.g. daydreaming). This lack of focus can contribute to the presence of non-task related activations. Also, every patient had background noise in their rooms, including music and television, during their

conversations. This increases the potential for additional artifacts in already difficult data.

It became clear data lost significant information during the ICA de-noising process, and this analysis was therefore dismissed.

Future Work

The next phase of this study is to generate 3-dimensional brain models containing accurate electrode placement; therefore, patient CT and MRI DICOMs must be procured. This would allow quantification of each method's detection ability. One area on which to focus is the calculation of individual speech condition latencies - it would be impossible to determine the correlation between functional activation latencies and cortical structures without the precise electrode location.

Also, the next researcher should be mindful of standardizing the data extraction protocol. As this study evolved, certain limitations necessitated that data were extracted differently for several patients. It was difficult to test all patients in the same way- the first four patients required the manual recording of exact times in which each speech condition changed throughout their conversations- which necessitated the use of the HT to estimate their power. P5's data were single epochs which allowed the use of a spectrogram to estimate power.

Further, since the results of the study are based on the comparison of speech segments to baseline, special attention should be given to the data that are chosen. A "good" baseline should involve as little activity as possible, and include an adequate amount (only a few seconds of baseline was available for several patients).

Another important step would be to demonstrate reproducibility. If the results of the experimental control were repeated for subsequent patients, this task (listening to words) may be considered a suitable alternative to DCS.

Finally, establishing a better relationship with the EMU technicians is a simple yet critical step in addressing data insufficiency. It should be clearly understood what data are required to remain on the hospital's server (for a reasonable amount of time) until data extraction. This would allow the reviewer to be more selective in their choice of data containing conversations (i.e. not during meals and patient is obviously engaged in conversation).

REFERENCES

- Anderson, J.M., Gilmore, R., Roper, S., Crosson, B., Bauer, R.M., Nadeau, S., Beversdorf, D.Q., Cibula, J., Rogish III, M., Kortencamp, S., Hughes, J.D., Gonzalez Rothi, L.J., and Heilman, K.M. (1999). Conduction Aphasia and the Arcuate Fasciculus: A Reexamination of the Wernicke–Geschwind Model. *Brain and Language*, 70(1): 1-12, ISSN: 0093-934X.
- Ball, T., Demandt, E., Mutschler, I., Neitzel, E., Mehring, C., Vogt, K., Aertsen, A., and Schulze-Bonhage, A. (2008). Movement related activity in the high gamma range of the human EEG. *NeuroImage*, 41(2): 302–310.
- Benbadis, S.R., LaFrance, W.C., Papandonatos, G.D., Korabathina, K., Lin K., and Kraemer, HC. (2009). Interrater reliability of EEG-video monitoring. *Neurology*, 73(11): 843–6. doi: 10.1212/WNL.0b013e3181b78425.
- Bernal, B., and Ardila, A. (2009). The role of the arcuate fasciculus in conduction aphasia, *Brain*, 132(9): 2309-2316. doi: 10.1093/brain/awp206.
- Blumenfeld, H., 2002, *Neuroanatomy through Clinical Cases*, Sinauer Associates, Sunderland, 951 p.
- Cervenka, M., Corines, J., Boatman-Reich, D., Eloyan, A., Sheng, X., Franaszczuk, P., and Crone, N. (2013). Electrographic functional mapping identifies human cortex critical for auditory and visual naming. *NeuroImage*, 69(3): 267–276. <http://dx.doi.org/10.1016/j.neuroimage.2012.12.037>.
- Cho-Hisamoto, Y., Kojima, K., Brown, E., Matsuzaki, N., and Asano, E. (2012). Cooing- and babbling-related gamma-oscillations during infancy: Intracranial recording. *Epilepsy & Behavior*, 23(2): 494–496.
- Crone, N., Boatman, D., Gordon, B., and Hao, L. (2001). Induced electrocorticographic gamma activity during auditory perception. Brazier Award-winning article, 2001. *Clin Neurophysiol*, 112(4): 565-582.
- Crone, N., Miglioretti, D., Gordon, B., and Lesser, R. (1998). Functional mapping of human sensorimotor cortex with electrocorticographic spectral analysis. II. Event-related synchronization in the gamma band. *Brain*, 121(12): 2301-2315.
- Dien, Joseph. (1998). Issues in the application of the average reference: Review, critiques, and recommendations. *Behavior Research Methods*, 30(1): 34-43.

Dronkers, N.F., Plaisant, O., Iba-Zizen, M.T., and Cabanis, E.A. (2007). Paul Broca's historic cases: high resolution MR imaging of the brains of Leborgne and Lelong. *Brain*, 130(5): 1432-1441. doi: 10.1093/brain/awm042.

Duffau H, Capelle L, Denvil D, Gatignol P, Sichez N, Lopes M, Sichez J P and Van Effenterre R. (2003). The role of dominant premotor cortex in language: a study using intraoperative functional mapping in awake patients. *Neuroimage*, 20(4): 1903–14.

Edwards, E., Nagarajan, S.S., Dalal, S.S., Canolty, R.T., Kirsch, H.E., Barbaro, N.M., and Knight, R.T. (2010). Spatiotemporal imaging of cortical activation during verb generation and picture naming. *NeuroImage*, 5(8): 291-301.

Epilepsy Foundation. (2012). Not another moment lost to seizures. Retrieved from: <<http://www.epilepsyfoundation.org/aboutepilepsy/>>.

Fridriksson, J., Bonilha, L., and Rorden, C. (2007). Severe Broca's aphasia without Broca's area damage. *Behavioural Neurology*, 18(4): 237-238.

Gerber, P.A., Chapman, K.E., Chung, S.S., Drees, C., Maganti R.K., Ng YT, et al. (2008). Interobserver agreement in the interpretation of EEG patterns in critically ill adults. *J Clin Neurophysiol*. 25(5): 241–9. doi: 10.1097/WNP.0b013e318182ed67.

Hanlon, R. E., Brown, J. W., and Gerstman, L. J. (1990). Enhancement of naming in nonfluent aphasia through gesture. *PubMed*, 38(2): 298-314. PMID: 2322814.

Haut, S.R., Berg, A.T., Shinnar, S., Cohen, H.W., Bazil, C.W., Sperling, M.R., et al. (2002). Interrater reliability among epilepsy centers: Multicenter study of epilepsy surgery. *Epilepsia*, 43(11): 1396–401. PMID: 12423391.

Hill, N., Gupta, D., Brunner, P., Gunduz, A., Adamo, M., Ritaccio, A., and Schalk, G. (2012). Recording human electrocorticographic (ECoG) signals for neuroscientific research and real-time functional cortical mapping. *J Vis Exp*, (64): 3993. doi: 10.3791/3993. PMID: 22782131.

Hyeok Gyu, K., and Sung Ho, J. (2011). Excellent recovery of aphasia in a patient with complete injury of the arcuate fasciculus in the dominant hemisphere. *NeuroRehabilitation*. 29(4): 401. ISSN: 1053-8135. PMID: 22207068.

Kellis, S., Miller, K., Thomson, K., Brown, R., House, P., and Greger, B. (2010). Decoding spoken words using local field potentials recorded from the cortical surface. *Journal of Neural Engineering*, 7(5): 1741-2560. doi: 10.1088/1741-2560/7/5/056007.

Leuthardt, E., Gaona, C., Sharma, M., Szrama, N., Roland, J., Freudenberg, Z., Solis, J., Breshears, J., Schalk, G. (2011). Using the electrocorticographic speech network to control a brain-computer interface in humans. *Journal of Neural Engineering*, 8(5): 1741-2560. doi:10.1088/1741-2560/8/3/036004.

- Leuthardt, E., Miller, K., Anderson, N., et al. (2007). Electrocorticographic frequency alteration mapping: a clinical technique for mapping the motor cortex. *Neurosurgery*, 60(4 suppl 2): 260-270; discussion 270-261.
- Liberman, A. M., Cooper, F. S., Shankweiler, D. P., and Studdert-Kennedy, M. (1967). Perception of the speech code. *Psychological Review*, 74(6): 431-461. doi: 10.1037/h0020279.
- Lodder, S. and J.A.M. van Putten, M. (2013). Quantification of the adult EEG background pattern. *Clinical neurophysiology*, 124(2): 228-237. PMID: 22917580. doi: 10.1016/j.clinph.2012.07.007.
- MATLAB version 7.10.0. Natick, Massachusetts: The MathWorks Inc., 2012.
- McCaffrey, Patrick. Specific Syndromes: Affluent Aphasias. (2008). The Neuroscience on the Web Series. Retrieved from: <<http://www.csuchico.edu/~pmccaffrey/syllabi/SPPA336/336unit8.html>>.
- McAndrew, R., Lingo VanGilder, J., Naufel, S., Helms Tillery, S.I. (2011). Individualized recording chambers for non-human primate neurophysiology, *Journal of Neuroscience Methods*, 207(1): 86-90. doi: 10.1016/j.jneumeth.2012.03.014.
- Pei, X., Barbour, L. D., Leuthardt, C. E., and Schalk, G. (2011). Decoding vowels and consonants in spoken and imagined words using electrocorticographic signals in humans. *Journal of Neural Engineering*, 8(4): 1741-2560. doi: 10.1088/1741-2560/8/4/046028.
- Ray, S., Niebur, E., Hsiao, S., Sinai, A., and Crone, N. (2008). High-frequency gamma activity (80-150Hz) is increased in human cortex during selective attention. *Clin Neurophysiol*, 119(1): 116-33. Epub 2007 Nov 26.
- Schachter, Steven. Symptoms of a Seizure. 2006. Epilepsy Therapy Project. Retrieved from: <http://www.epilepsy.com/101/EP101_SYMPTOM>.
- Selnes, O.A., C.M., P., van Zijl, Barker, P., Hillis, A., and Mori, S. (2010). MR diffusion tensor imaging documented arcuate fasciculus lesion in a patient with normal repetition performance. *Aphasiology*, 16(9): 897-902. doi: 10.1080/02687030244000374.
- Sinai, A., Bowers, C., Crainiceanu, C., Boatman, D., Gordon, B., Lesser, R., Lenz F., and Crone, N. (2005). Electrocorticographic high gamma activity versus electrical cortical stimulation mapping of naming. *Brain*, 128(7): 1556–1570.
- Sun, F., Morrell, M., and Wharen, R. (2007). Responsive cortical stimulation for the treatment of epilepsy. *Neurotherapeutics*, 5(1): 68-74. doi:10.1016/j.nurt.2007.10.069.

Topper, R., Mottaghy, F. M., Brugmann, M., Noth, J., and Huber, W. (1998). Facilitation of picture naming by transcranial magnetic stimulation of Wernicke's area. *Experimental Brain Research*, 121(4): 371-378.

Towle, V. L., Yoon, H. A., Castelle, M., Edgar, J. C., Biassou, N. M., Frim, D. M., Spire, J. P., and Kohrman, M.H. (2008). ECoG Gamma activity during a language task: differentiating expressive and receptive speech areas. *Brain*, 131(8): 2013-2027. doi: 10.1093/brain/awn147.

Weiner, Howard. Surgery. (2004). Epilepsy Therapy Project. Retrieved from: <<http://www.epilepsy.com/EPILEPSY/surgery>>.

Weisman, D., Hisama, F.M., Waxman, S.G., and Blumenfeld, H. (2003). Going deep to cut the link: Cortical disconnection syndrome caused by a thalamic lesion. *Neurology*, 60(11): 1865-1866. doi: 10.1212/01.WNL.0000066051.14414.FF.

World Health Organization. (2012). Epilepsy. Retrieved from: <<http://www.who.int/mediacentre/factsheets/fs999/en/>>.

Wilson, S. M., Saygin, A. E. P., Sereno, M. I., and Iacoboni, M. (2004). Listening to speech activates motor areas involved in speech production. *Nature Neuroscience*, 7(7): 701-702.

Wise, R., Scott, S., Blank, S., Mummery, C., Murphy, K., and Warburton, E. (2001). Separate neural subsystems within 'Wernicke's area'. *Brain*, 124(1): 83-95. PMID: 11133789.

Wu, M., Wisneski, K., Schalk, G., Sharma, M., Roland, J., Breshears, J., Gaona, C., and Leuthardt, E. (2010). Electrocorticographic Frequency Alteration Mapping for Extraoperative Localization of Speech Cortex. *Neurosurgery*, 66(2): E407-E409. doi: 10.1227/01.NEU.0000345352.13696.6F

APPENDIX I

BRAIN SKETCHES OF SIGNIFICANT ACTIVATIONS

Figure 6. Patient 1 Brain Sketch Segments

31

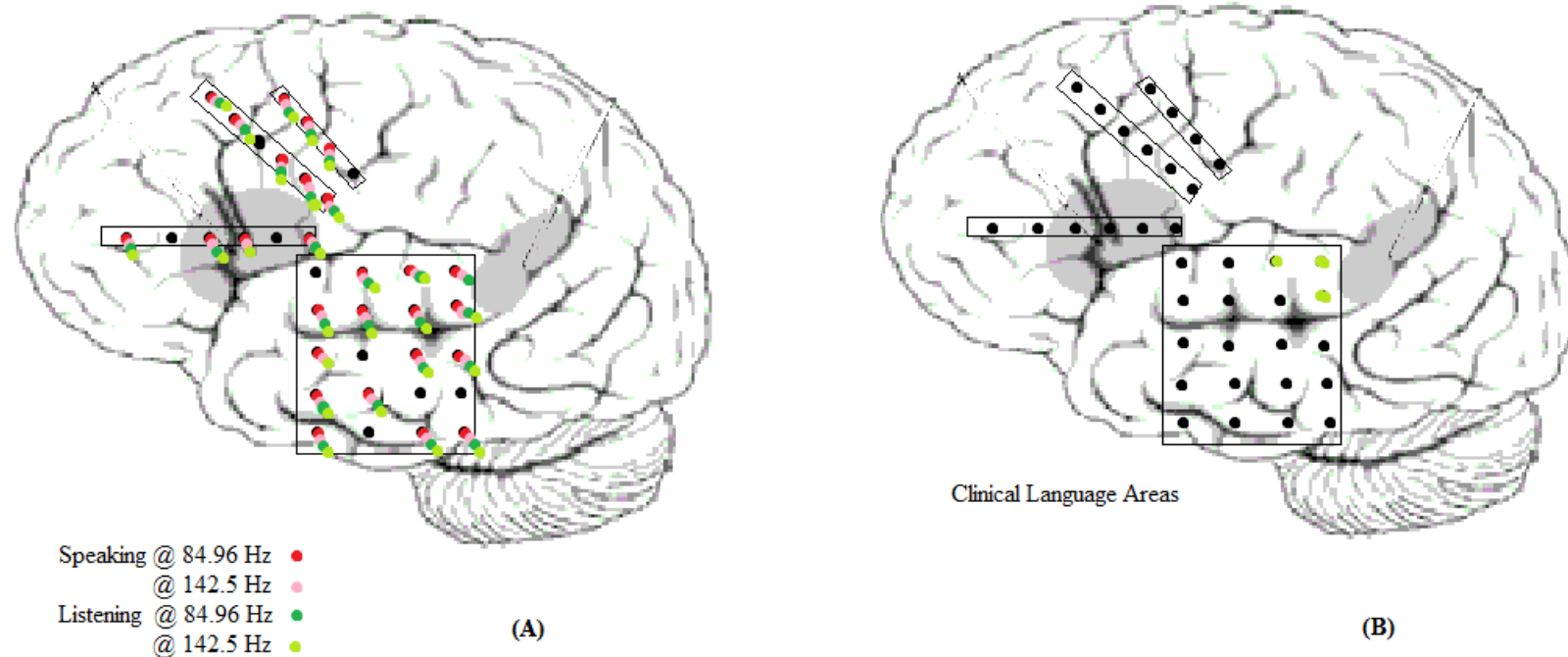


Figure 6: Two brains with electrodes found to be language-specific. Brain (A) illustrates widespread statistically significant electrode activations during both listening and speaking conditions for Patient 1. The power of each language condition was estimated by the HT from the above frequencies and separated into similar segments; speaking and listening were then compared to baseline. The black electrodes were removed from analysis (dead channel or contained prominent seizure activity). Notice every contact was activated for both conditions except listening at 84.96 Hz in suspected Broca's area and primary auditory cortex, nor listening at 142.5 Hz near Wernicke's area. Again, grid locations are estimated from cross-referencing CT images with patient reports.

Figure 7. Patient 1 Brain Sketch Segments (Frequency Ranges)

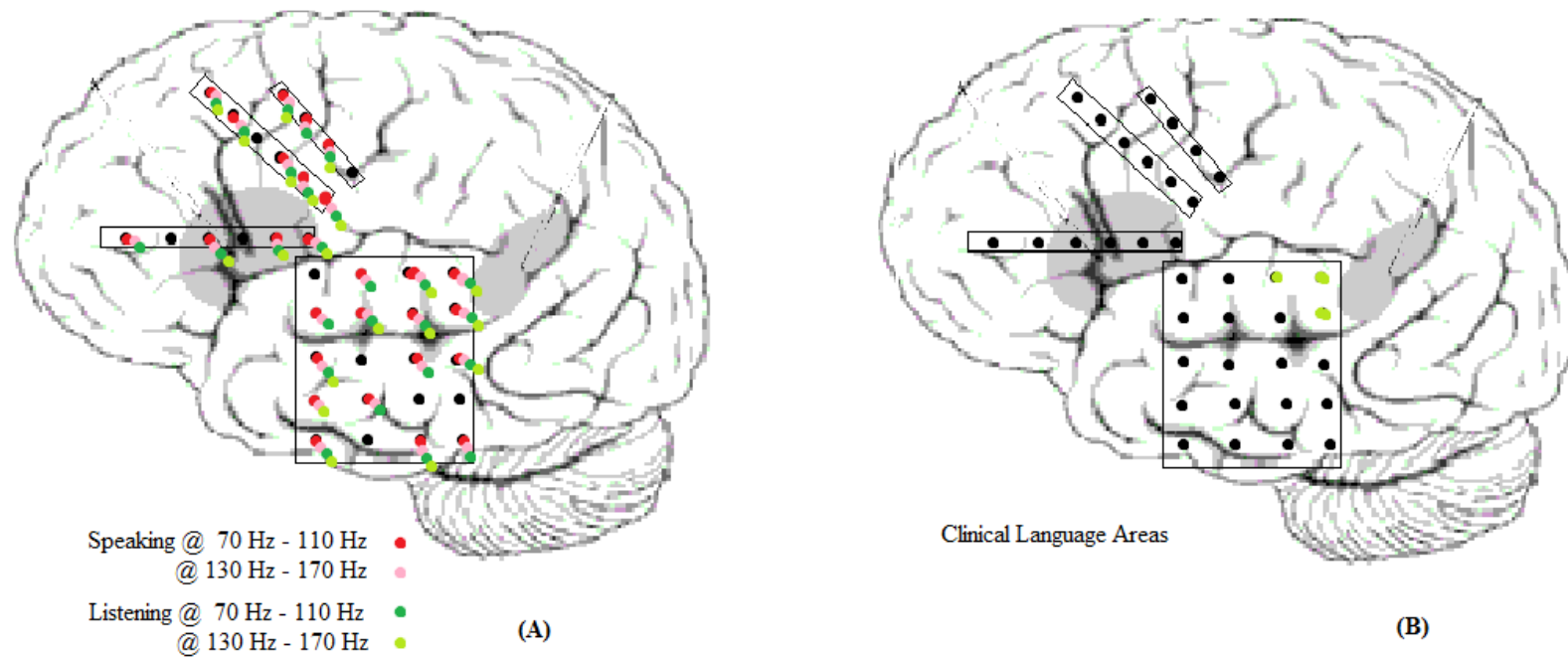


Figure 7: Two brains with electrodes found to be language-specific. Brain (A) illustrates widespread statistically significant electrode activations during both listening and speaking conditions for Patient 1. The power of each language condition was estimated by the HT from the above frequencies and separated into similar segments; speaking and listening were then compared to baseline. The black electrodes were removed from analysis (dead channel or contained prominent seizure activity). Notice every contact was activated for both conditions except listening at 142.5 Hz in anterior STG and frontal lobe. Again, grid locations are estimated from cross-referencing CT images with patient reports.

Figure 8. Patient 1 Brain Sketch Ratios

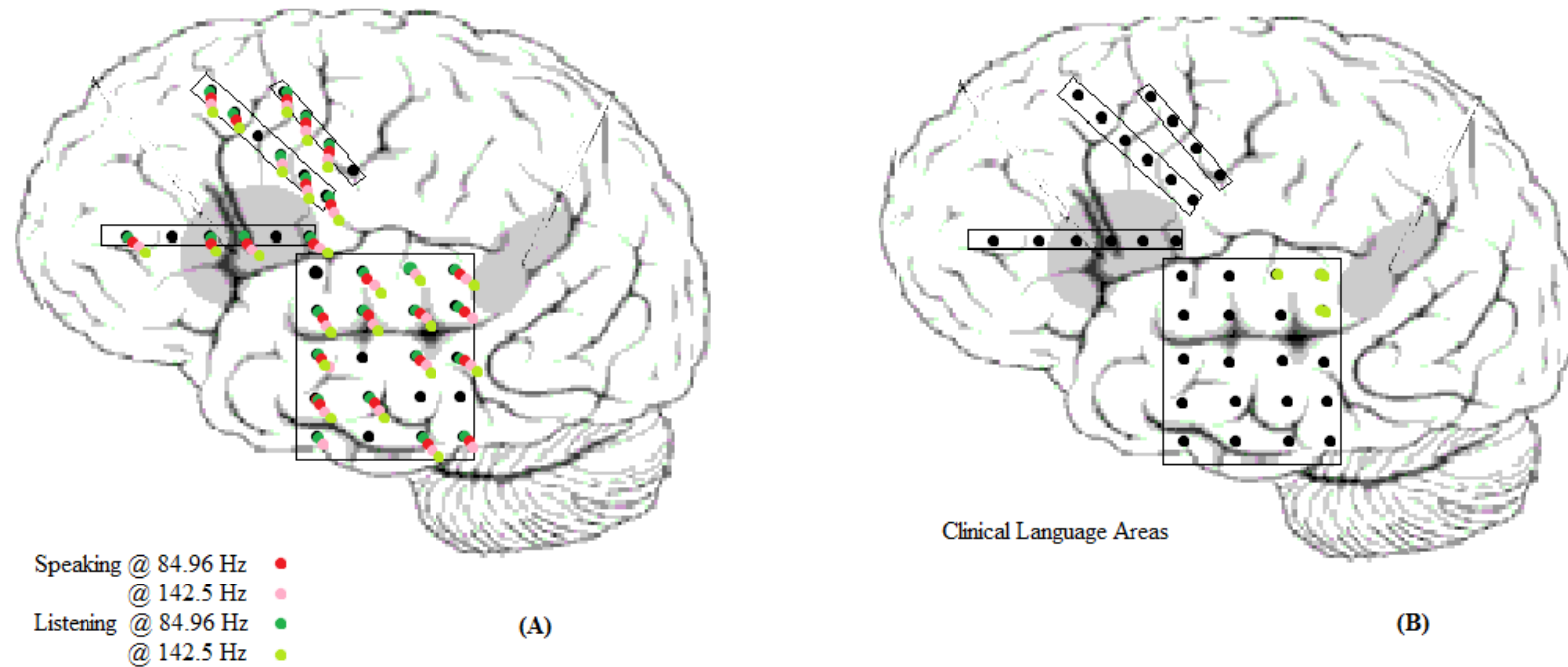


Figure 8: Two brains with electrodes found to be language-specific. Brain (A) illustrates widespread statistically significant electrode activations during listening and speaking conditions for Patient 1. The power of each language condition was estimated by the HT from the above frequencies and separated into similar segments; each condition was then divided by the averaged baseline. The power ratios of speaking and listening were then compared to normalized baseline. The black electrodes were removed from analysis (dead channel or contained prominent seizure activity).

Figure 9. Patient 1 Brain Sketch Ratios (Frequency Ranges)

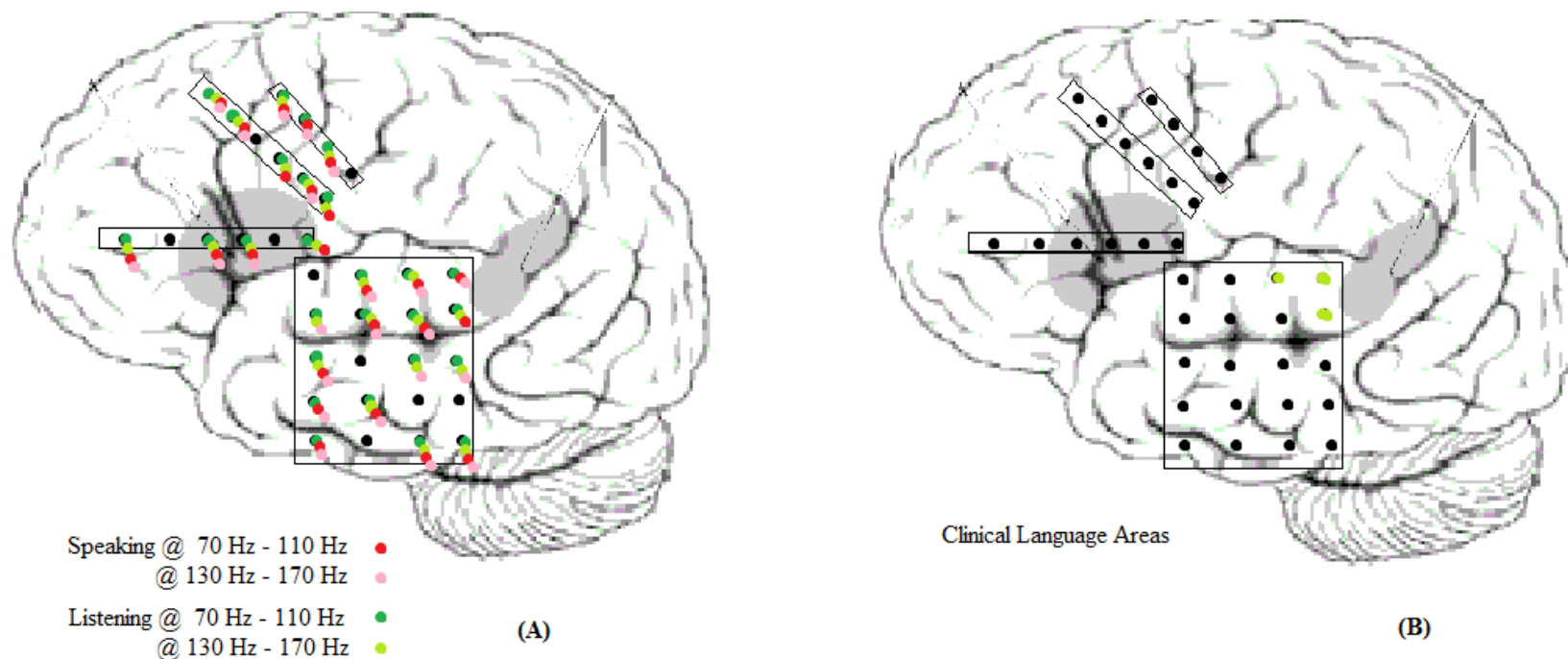


Figure 9: Two brains with electrodes found to be language-specific. Brain (A) illustrates widespread statistically significant electrode activations during listening and speaking conditions for Patient 1. The power of each language condition was estimated by the HT from the above frequencies and separated into similar segments; each condition was then divided by the averaged baseline. The power ratios of speaking and listening were then compared to normalized baseline. The black electrodes were removed from analysis (dead channel or contained prominent seizure activity).

Figure 10. Patient 1 Brain Sketch Combined Speech (Segments)

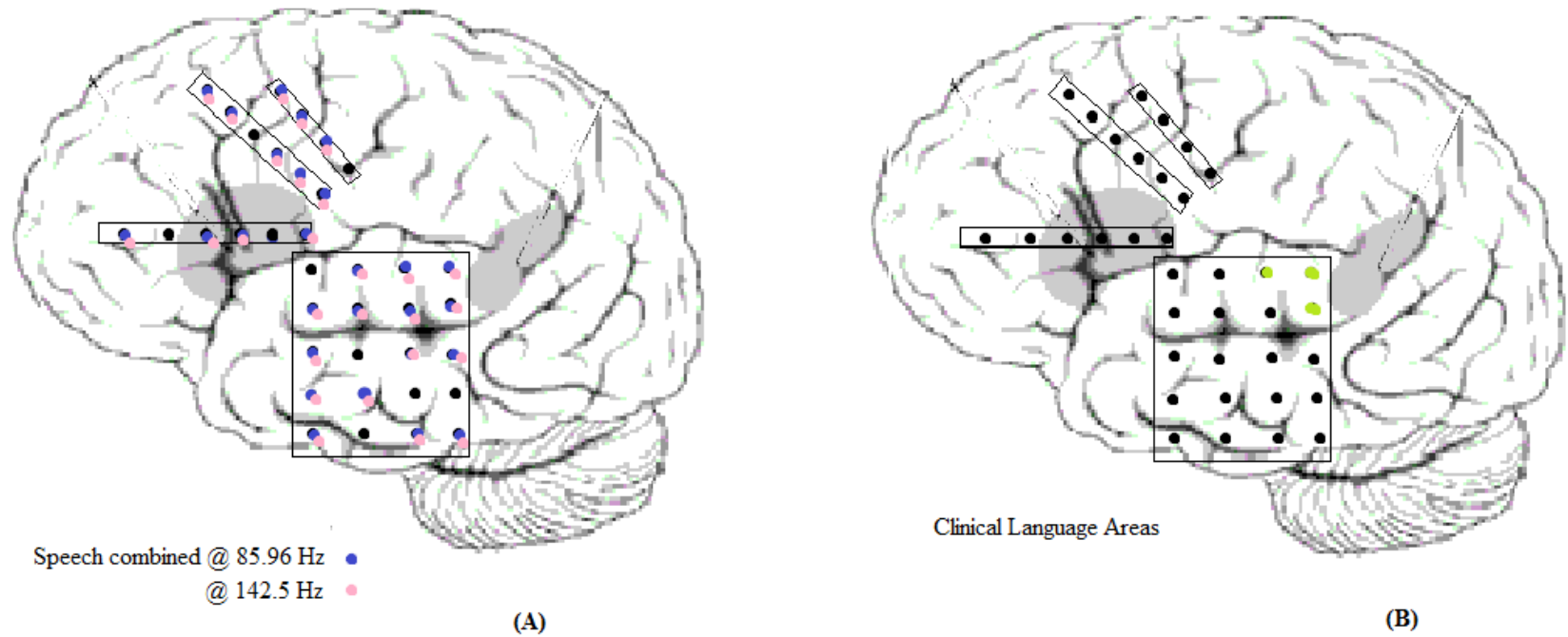


Figure 10: Two brains with electrodes found to be language-specific. Brain (A) illustrates widespread statistically significant electrode activations during combined speech conditions for Patient 1 over the left temporal and frontal lobes. The power of each language condition was estimated from the above specified frequencies and separated from baseline segments; the combined speech segments were then compared to baseline. Notice the power for both frequencies are significantly different than baseline for all electrodes (black electrodes were removed from analysis), except immediately inferior STG at 84.96 Hz.

Figure 11. Patient 1 Brain Sketch Combined Speech (Ratios)

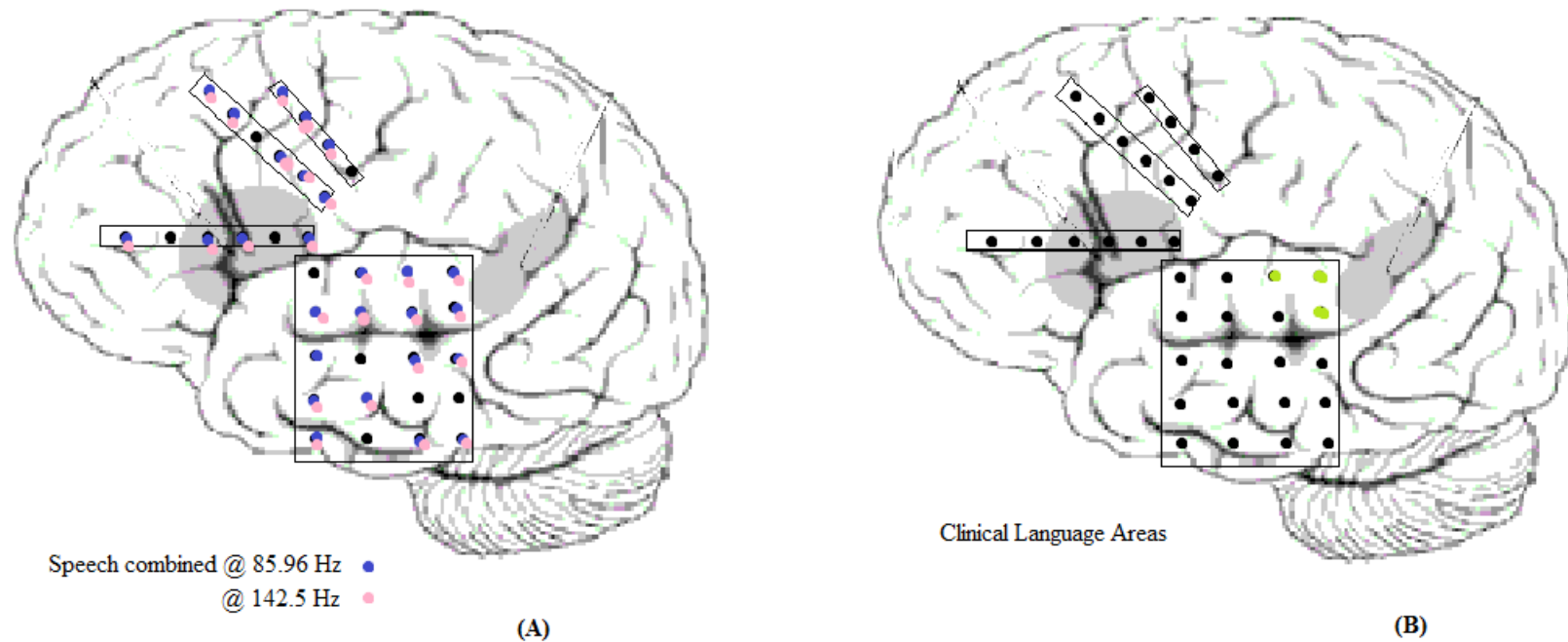


Figure 11: Two brains with electrodes found to be language-specific. Brain (A) illustrates widespread statistically significant electrode activations during listening and speaking conditions for Patient 1. The power of each language condition was estimated by the HT from the above frequencies and separated into similar segments; each condition was then divided by the averaged baseline. The power ratios of speaking and listening were then compared to normalized baseline. The black electrodes were removed from analysis (dead channel or contained prominent seizure activity). Notice all channels were activated for both frequencies except immediately inferior STG at 142.5 Hz.

Figure 12. Patient 2 Brain Sketch Segments

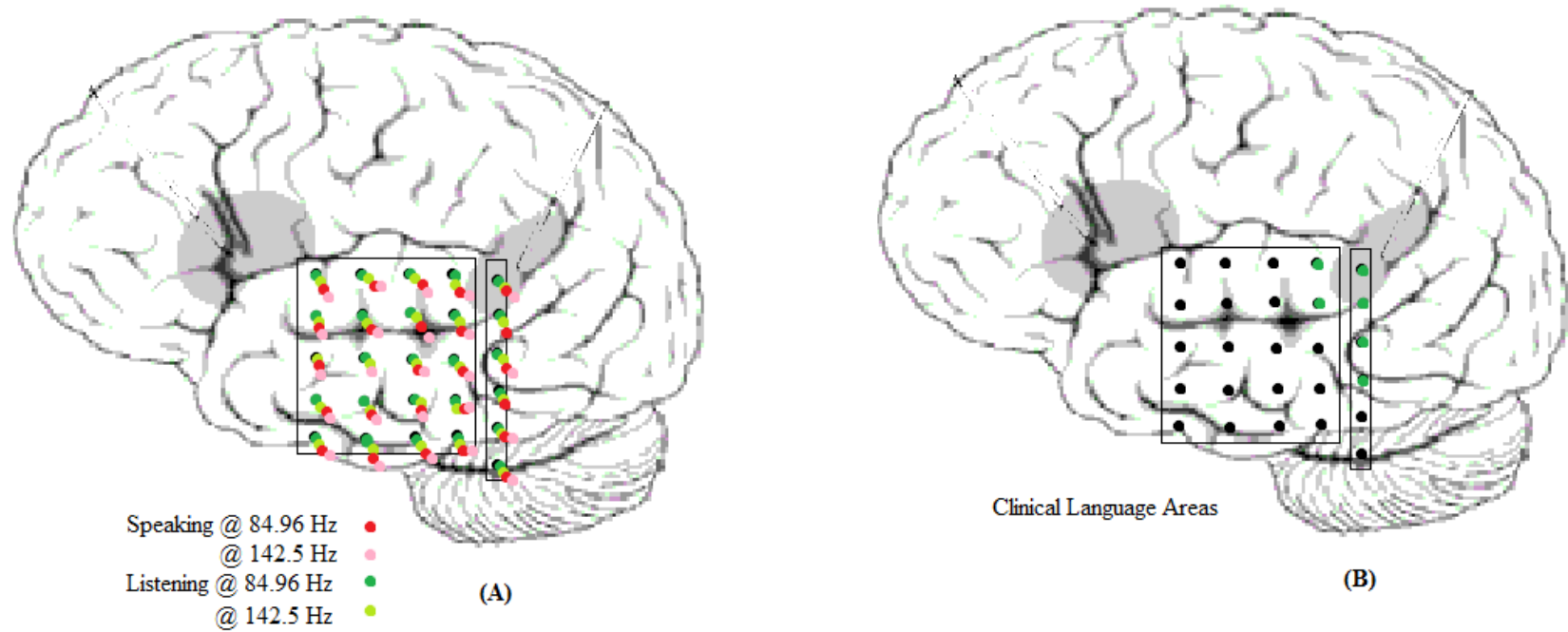


Figure 12: Two brains with electrodes found to be language-specific. Brain (A) illustrates widespread statistically significant electrode activations during both listening and speaking conditions for Patient 2 over the temporal lobe. The power of each language condition was estimated by the HT from the above frequencies and separated into similar segments; speaking and listening were then compared to baseline. The black electrodes were removed from analysis (dead channel or contained prominent seizure activity). Notice every electrode is activated for both speech conditions, except speaking at 142.5 Hz over the most posterior part of the temporal lobe.

Figure 13. Patient 2 Brain Sketch Segments (Frequency Ranges)

38

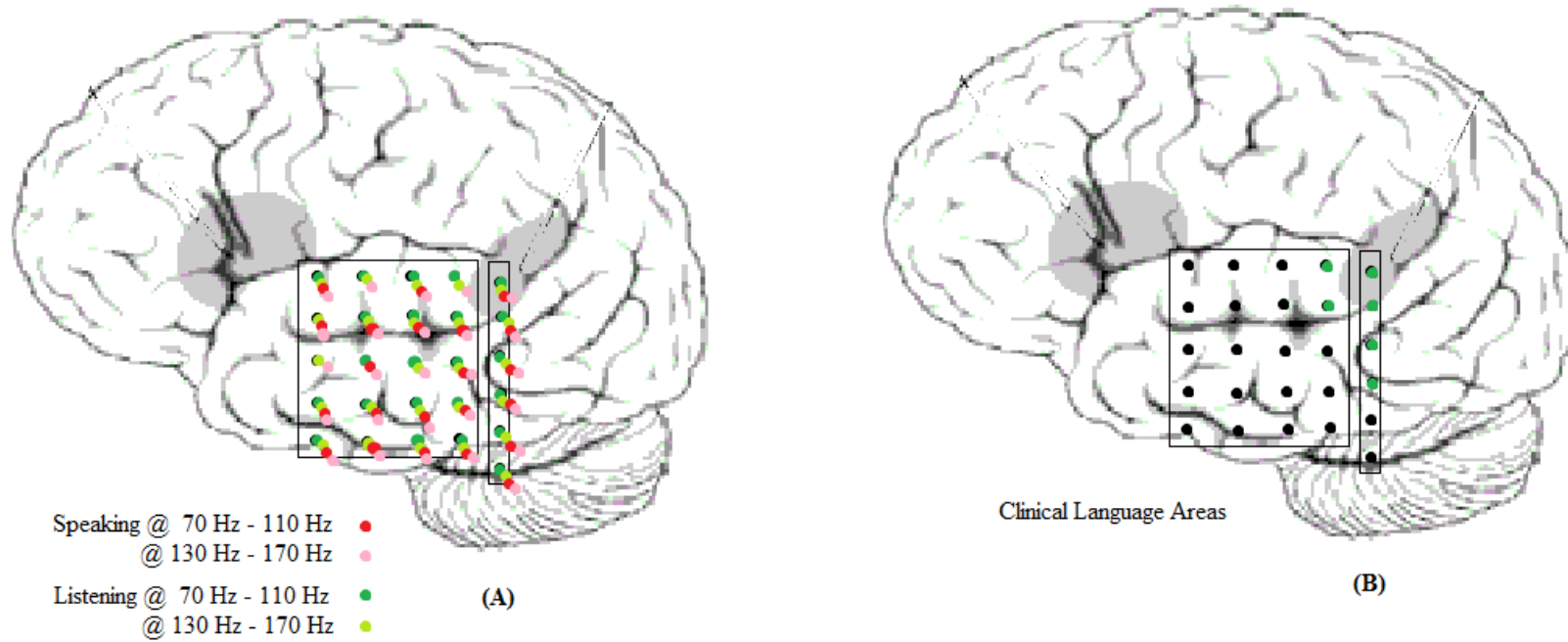


Figure 13: Two brains with electrodes found to be language-specific. Brain (A) illustrates widespread statistically significant electrode activations during both listening and speaking conditions for Patient 2 over the temporal lobe. The power of each language condition was estimated by the HT from the above frequencies and separated into similar segments; speaking and listening were then compared to baseline.

Figure 14. Patient 2 Brain Sketch Ratios

39

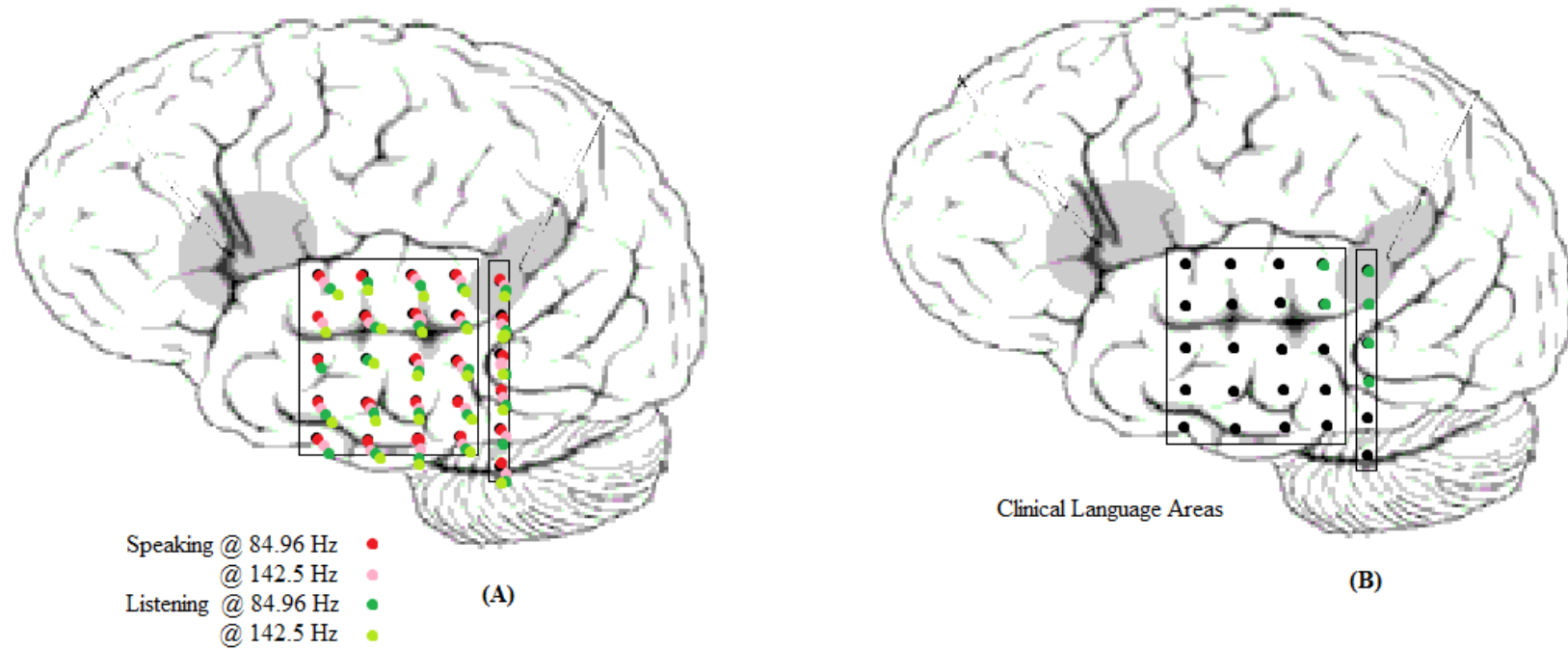


Figure 14: Two brains with electrodes found to be language-specific. Brain (A) illustrates widespread statistically significant electrode activations during listening and speaking conditions for Patient 2 over the temporal lobe. The power of each language condition was estimated by the HT from the above frequencies and separated into similar segments; each condition was then divided by the averaged baseline. The power ratios of speaking and listening were then compared to normalized baseline. Notice the posterior temporal lobe is activated during both conditions- for all frequencies, while the anterior part shows slight discrimination.

Figure 15. Patient 2 Brain Sketch Ratios (Frequency Ranges)

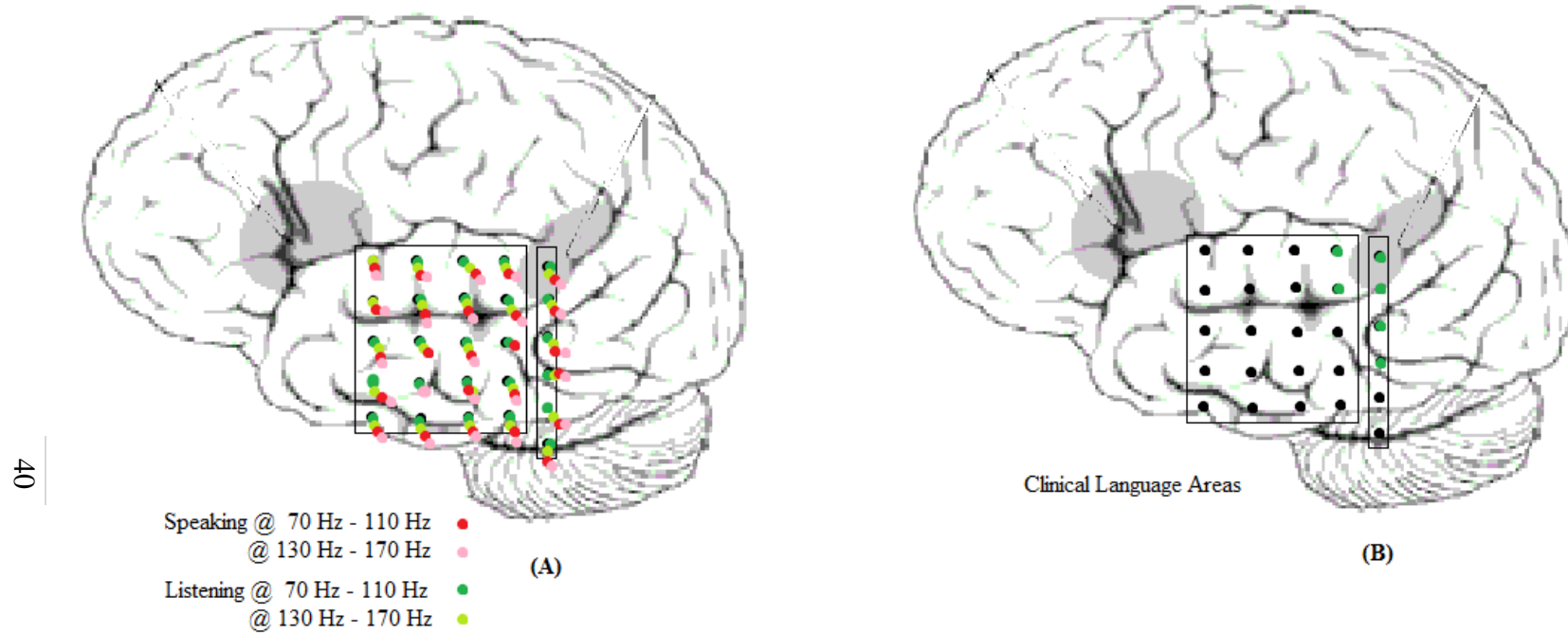


Figure 15: Two brains with electrodes found to be language-specific. Brain (A) illustrates widespread statistically significant electrode activations during listening and speaking conditions for Patient 2. The power of each language condition was estimated by the HT from the above frequencies and separated into similar segments; each condition was then divided by the averaged baseline. The power ratios of speaking and listening were then compared to normalized baseline. Notice listening at 84.96 Hz was significantly different from baseline throughout the entire grid except at the two most superior rostral electrodes.

Figure 16. Patient 2 Brain Sketch Combined Speech (Segments)

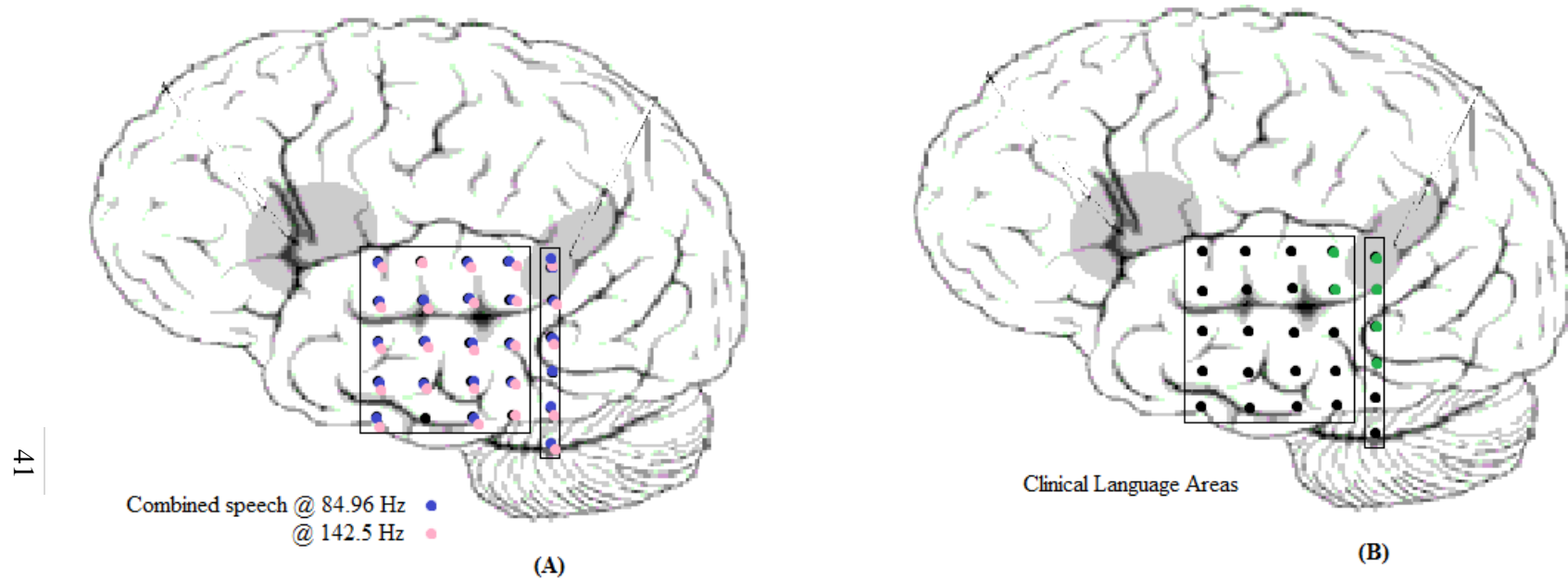


Figure 16: Two brains with electrodes found to be language-specific. Brain (A) illustrates widespread statistically significant electrode activations during combined speech conditions for Patient 2 over the left temporal lobe. The power of each language condition was estimated from the above specified frequencies and separated from baseline segments; the combined speech segments were then compared to baseline. Notice the power for both frequencies are significantly different than baseline for all electrodes, except one near the most inferior part of the temporal lobe.

Figure 17. Patient 2 Brain Sketch Combined Speech (Ratios)

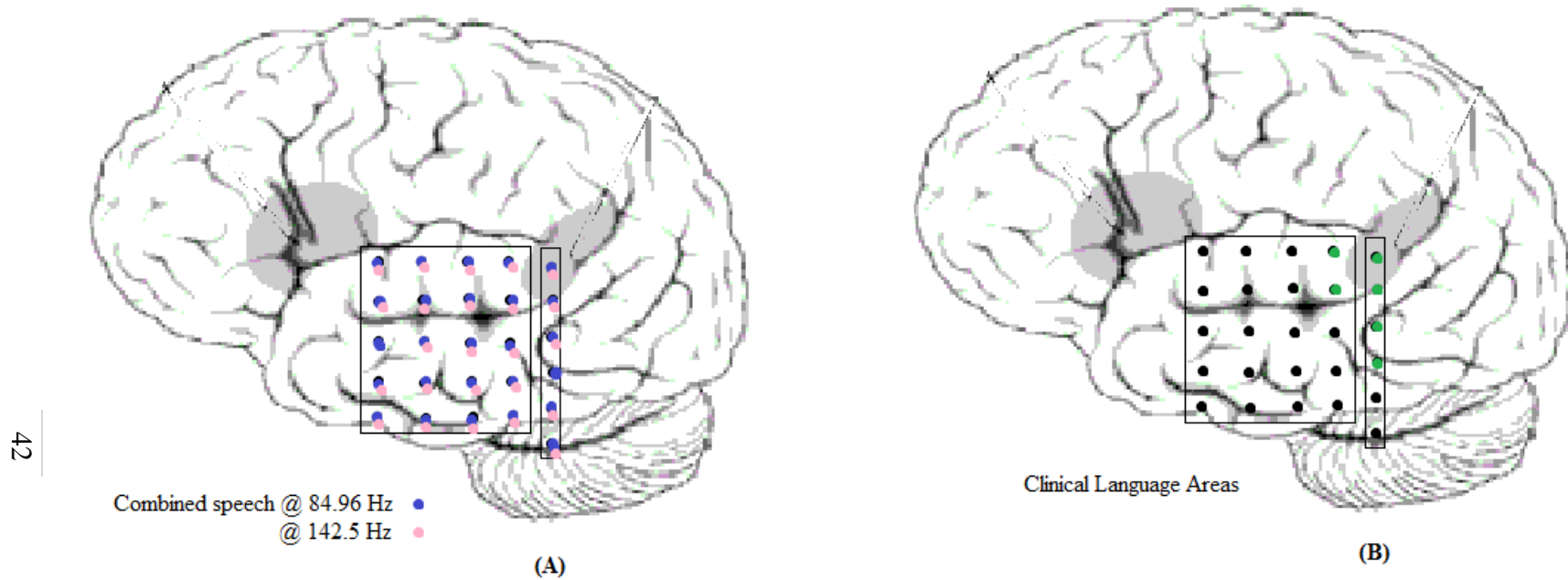


Figure 17: Two brains with electrodes found to be language-specific. Brain (A) illustrates widespread statistically significant electrode activations during listening and speaking conditions for Patient 2 over the temporal lobe. The power of each language condition was estimated by the HT from the above frequencies and separated into similar segments; each condition was then divided by the averaged baseline. The power ratios of speaking and listening were then compared to normalized baseline

Figure 18. Patient 3 Brain Sketch Segments

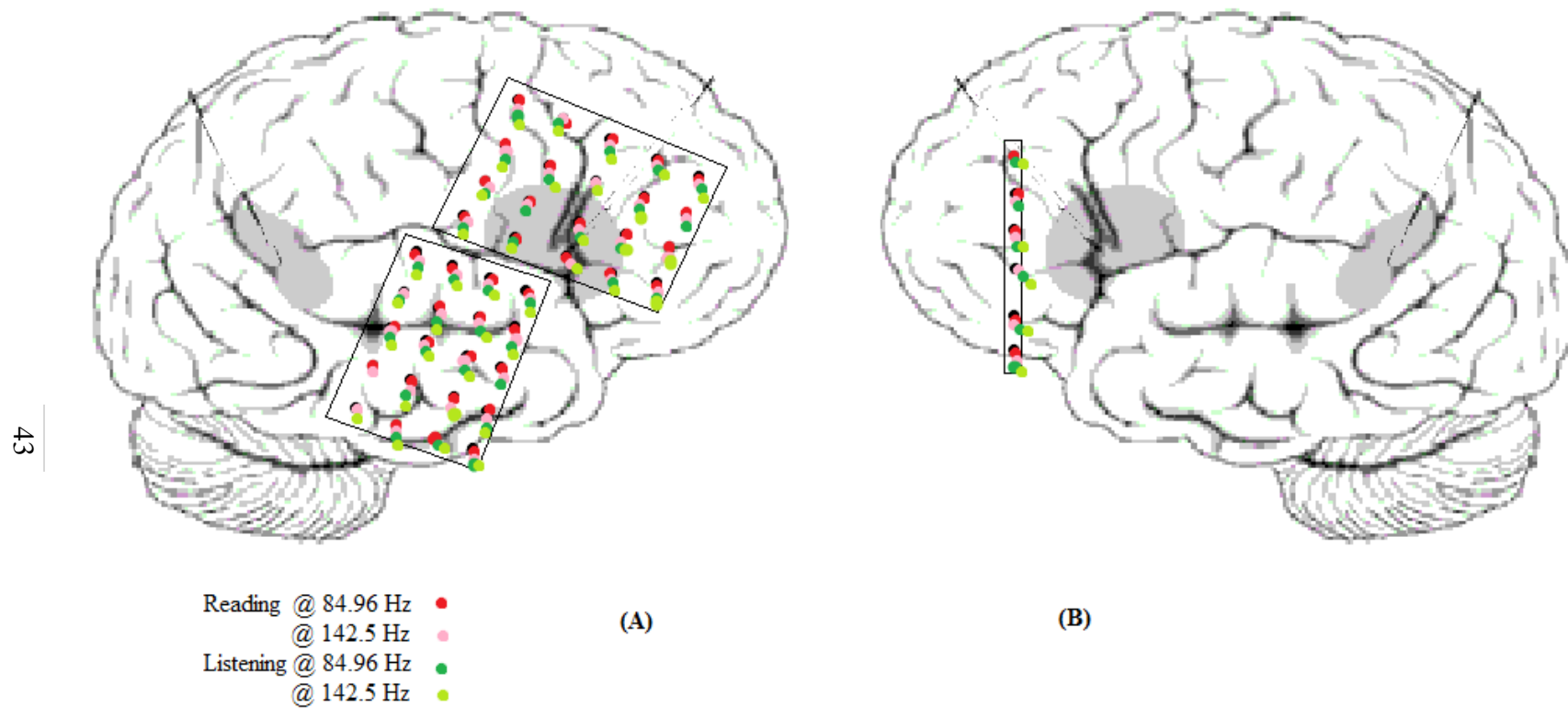


Figure 18: the left and right brain of Patient 3 with electrodes found to be language-specific; clinically-determined bilateral language areas (reading task) via fMRI. The power of each language condition was estimated from the above frequencies and separated into similar segments. Reading and listening were then compared to baseline. Both brains show broad frontal and temporal lobe activity.

Figure 19. Patient 3 Brain Sketch Segments (Frequency Ranges)

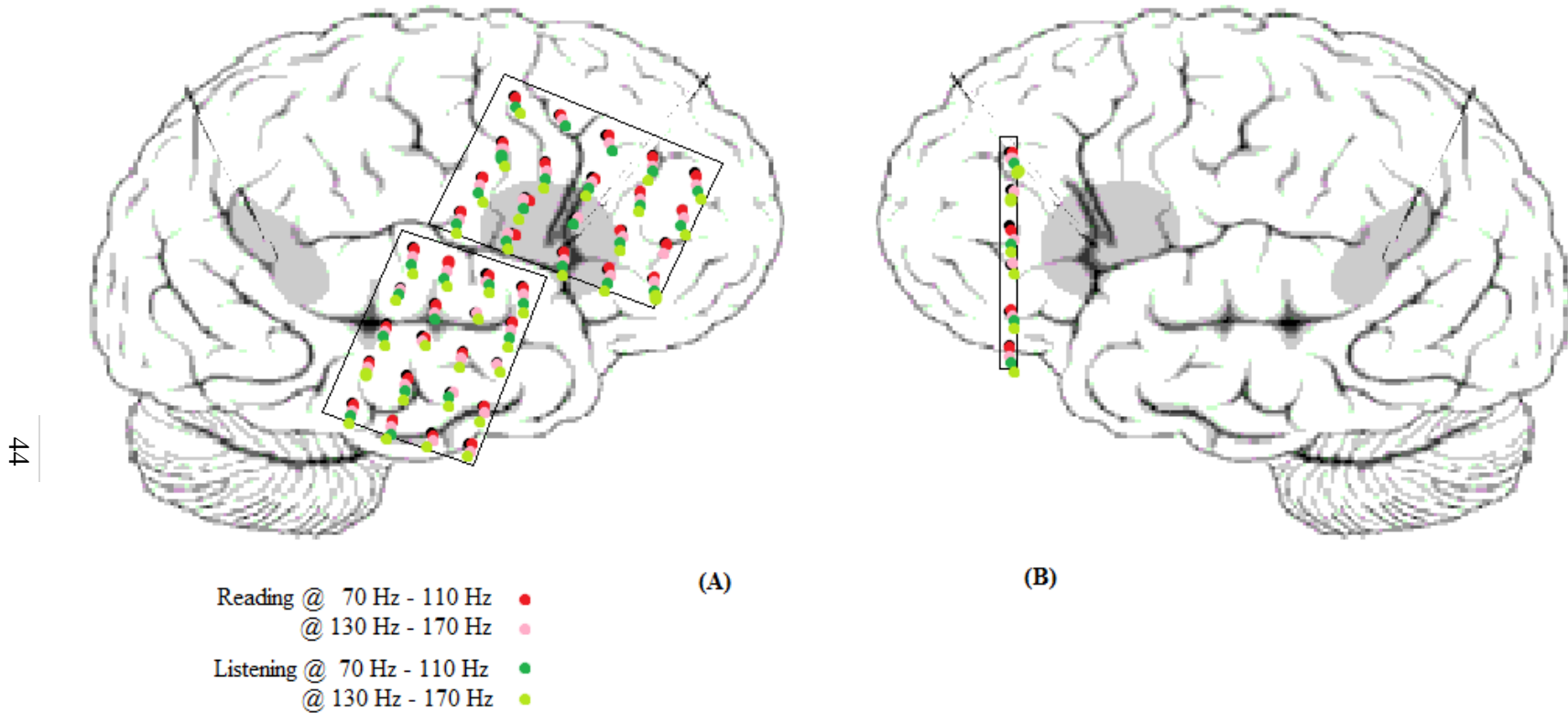


Figure 19: Left and right brain of Patient 3 with electrodes found to be language-specific; clinically-determined bilateral language areas (reading task) via fMRI. The power of each language condition was estimated from the above frequencies and separated into similar segments. Reading and listening were then compared to baseline. Notice broad activations except during reading near primary auditory cortex as well as Broca's area. Power during listening (@ 70 Hz to 110 Hz) is similar during baseline throughout the temporal grid, specifically near the primary auditory cortex.

Figure 20. Patient 3 Brain Sketch Ratios

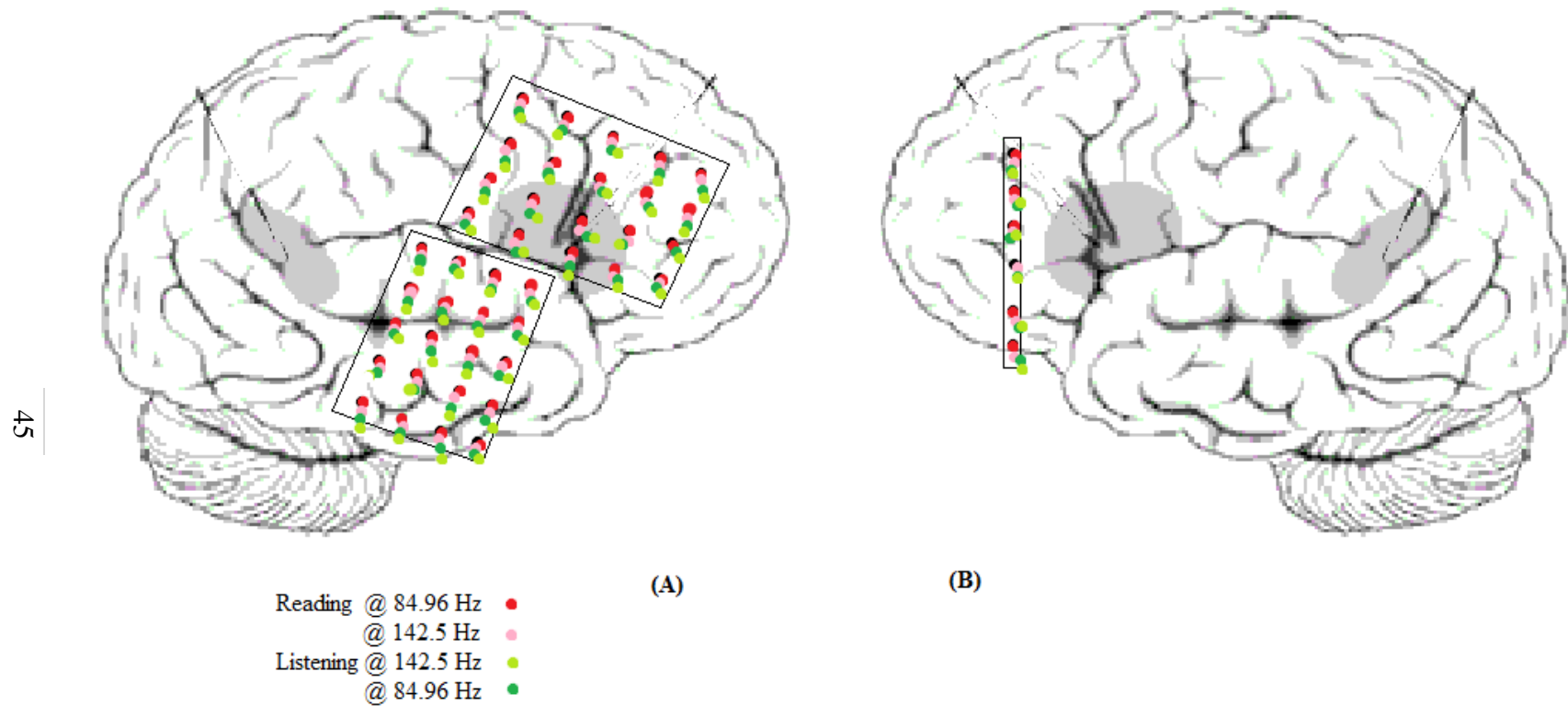


Figure 20: Left and right brain of Patient 3 with electrodes found to be language-specific; clinically-determined bilateral language areas (reading task) via fMRI. The power of each language condition was estimated from the above specified frequencies and separated into similar segments; each condition was then divided by the averaged baseline. Power ratios of reading and listening were compared to normalized baseline. Notice widespread activation throughout the right temporal and frontal cortices.

Figure 21. Patient 3 Brain Sketch Ratios (Frequency Ranges)

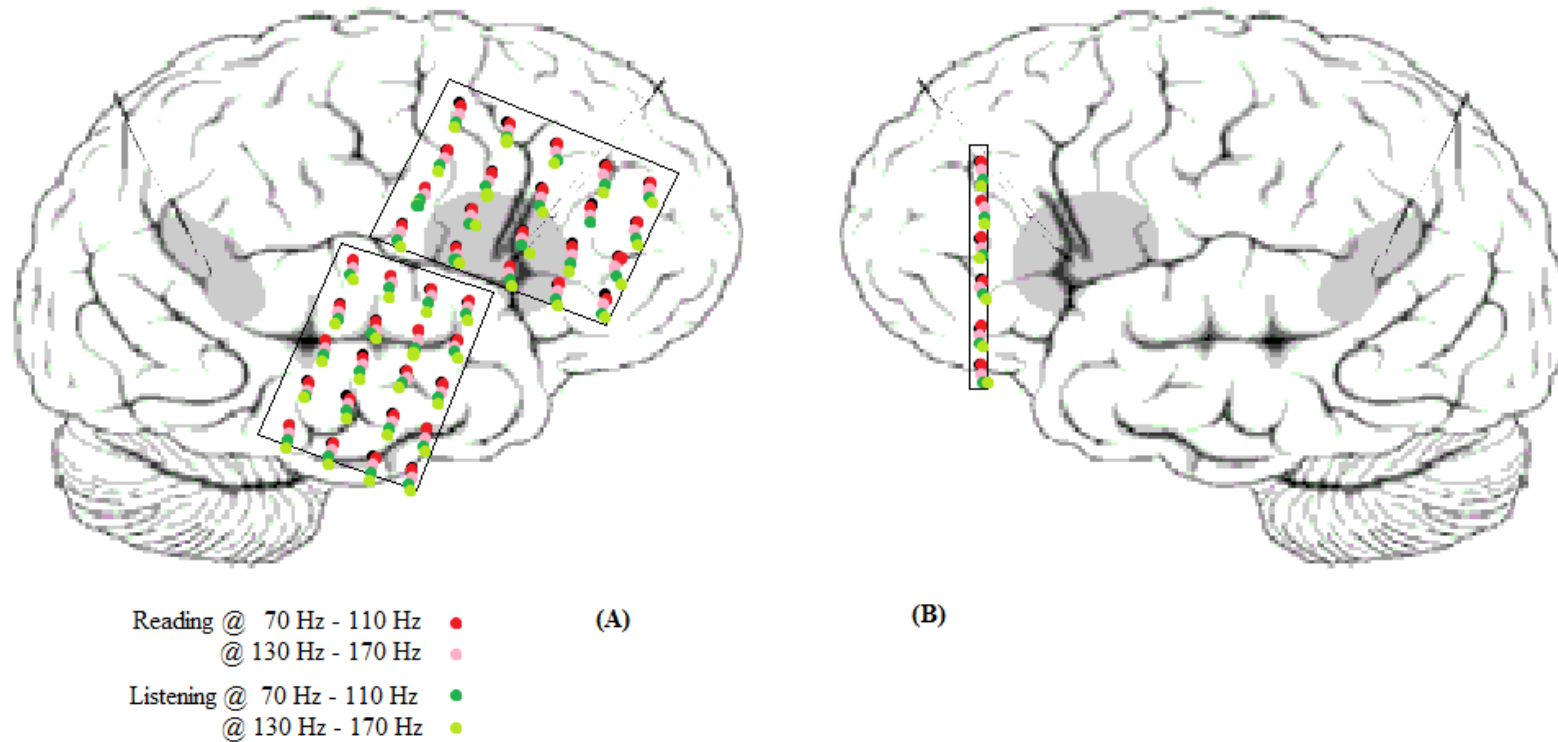


Figure 21: Left and right brain of Patient 3 with electrodes found to be language-specific; clinically-determined bilateral language areas (reading task) via fMRI. The power of each language condition was estimated from the above specified frequencies and separated into similar segments; each condition was then divided by the averaged baseline. Power ratios of reading and listening were compared to normalized baseline.

Figure 22. Patient 3 Brain Sketch Combined Speech (Segments)

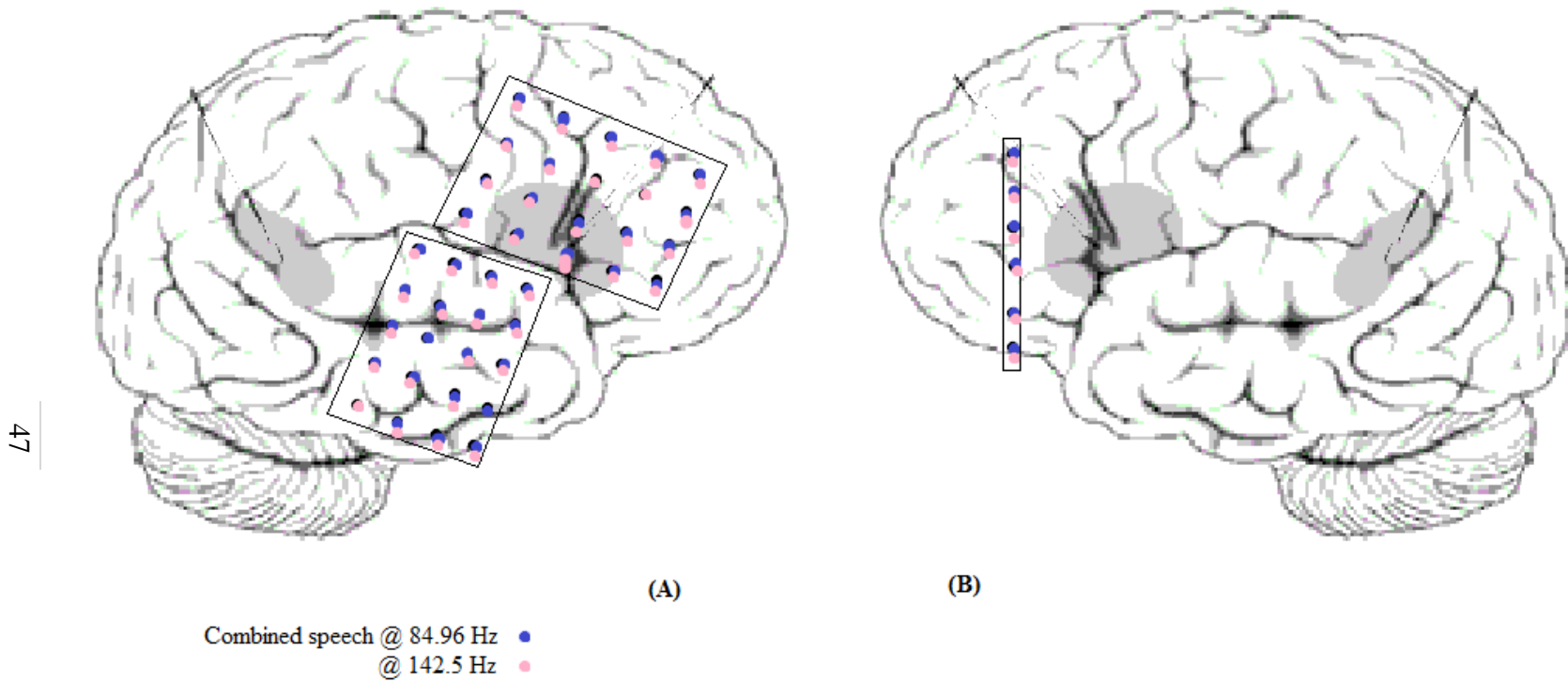


Figure 22: Left and right brains with electrodes found to be language-specific, these illustrate statistically significant electrode activations for listening and reading combined for Patient 3. The power of each language condition was estimated from the above specified frequencies and separated from baseline segments; the combined speech segments were then compared to baseline power. Notice two adjacent electrodes near suspected Broca's area are activated for combined speech at 142.5 Hz only.

Figure 23. Patient 3 Brain Sketch Combined Speech (Ratios)

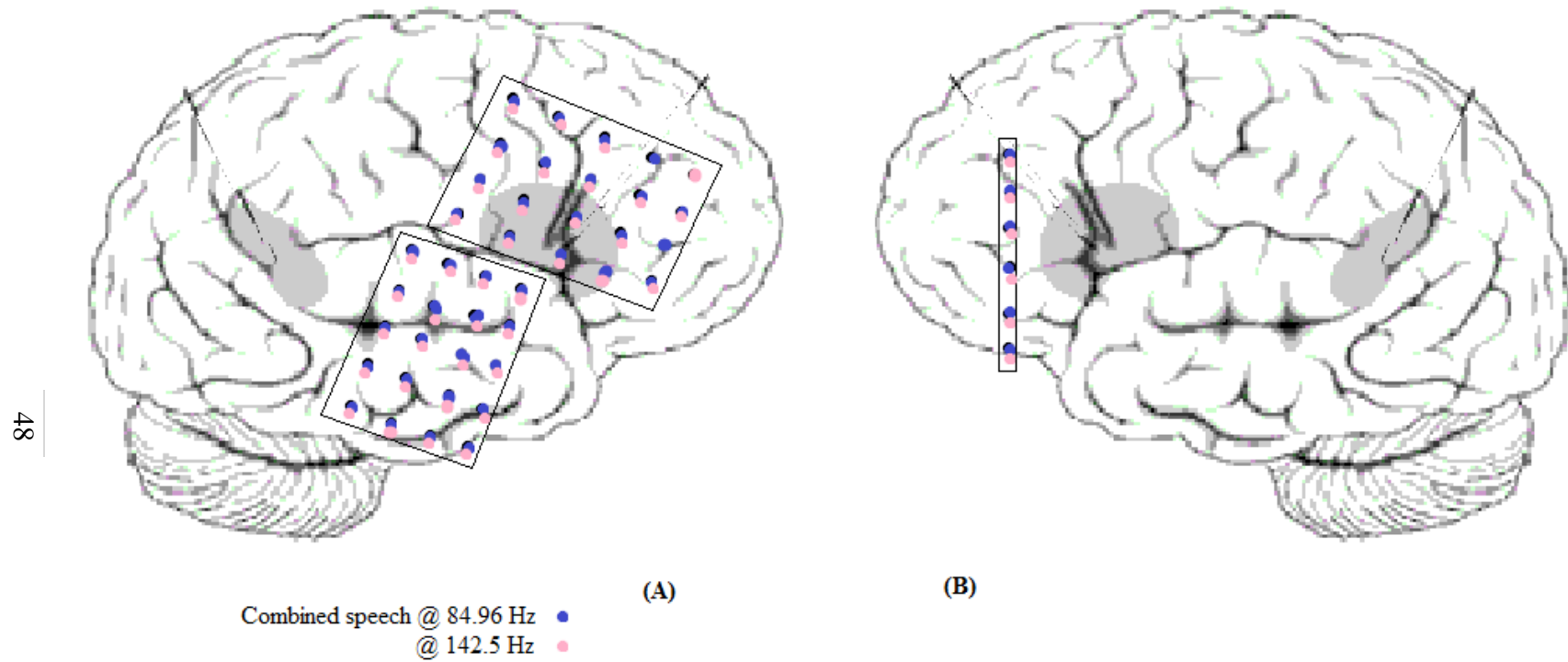


Figure 23: Left and right brain of Patient 3 with electrodes found to be language-specific; clinically-determined bilateral language areas (reading task) via fMRI. The power of each language condition was estimated from the above specified frequencies and separated into similar segments; each condition was then divided by the averaged baseline. The power ratios of reading and listening were combined and compared to the baseline ratio.

Figure 24. Patient 4 Brain Sketch Segments

49

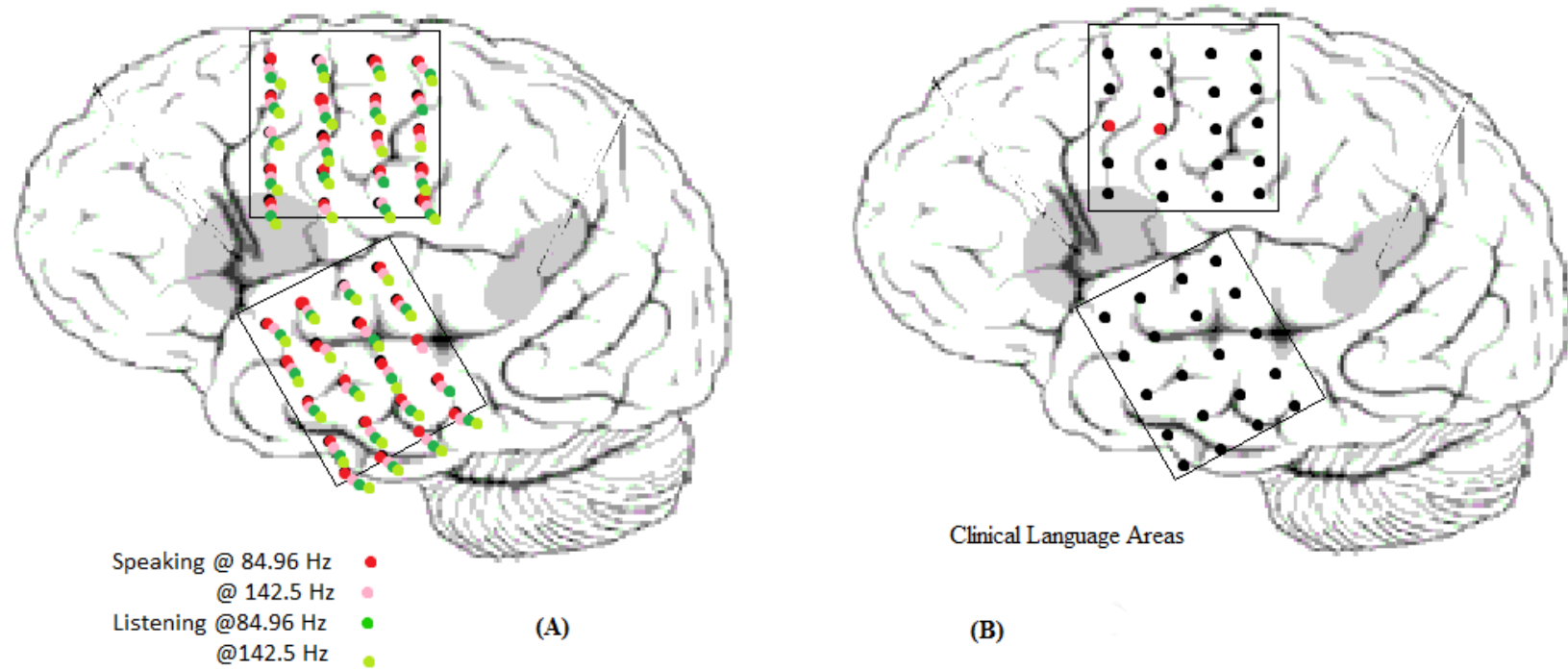


Figure 24: Two brains with electrodes found to be language-specific. The brain on the left illustrates statistically significant electrode activations during speaking and listening conditions for Patient 4 over the left temporal grid and estimated motor area (cross-referenced from CT images). The power of each language condition was estimated from the above frequencies and separated into similar segments. Speaking and listening were then compared to baseline. Notice widespread activation across the temporal and motor cortices.

Figure 25. Patient 4 Brain Sketch Segments (Frequency Ranges)

50

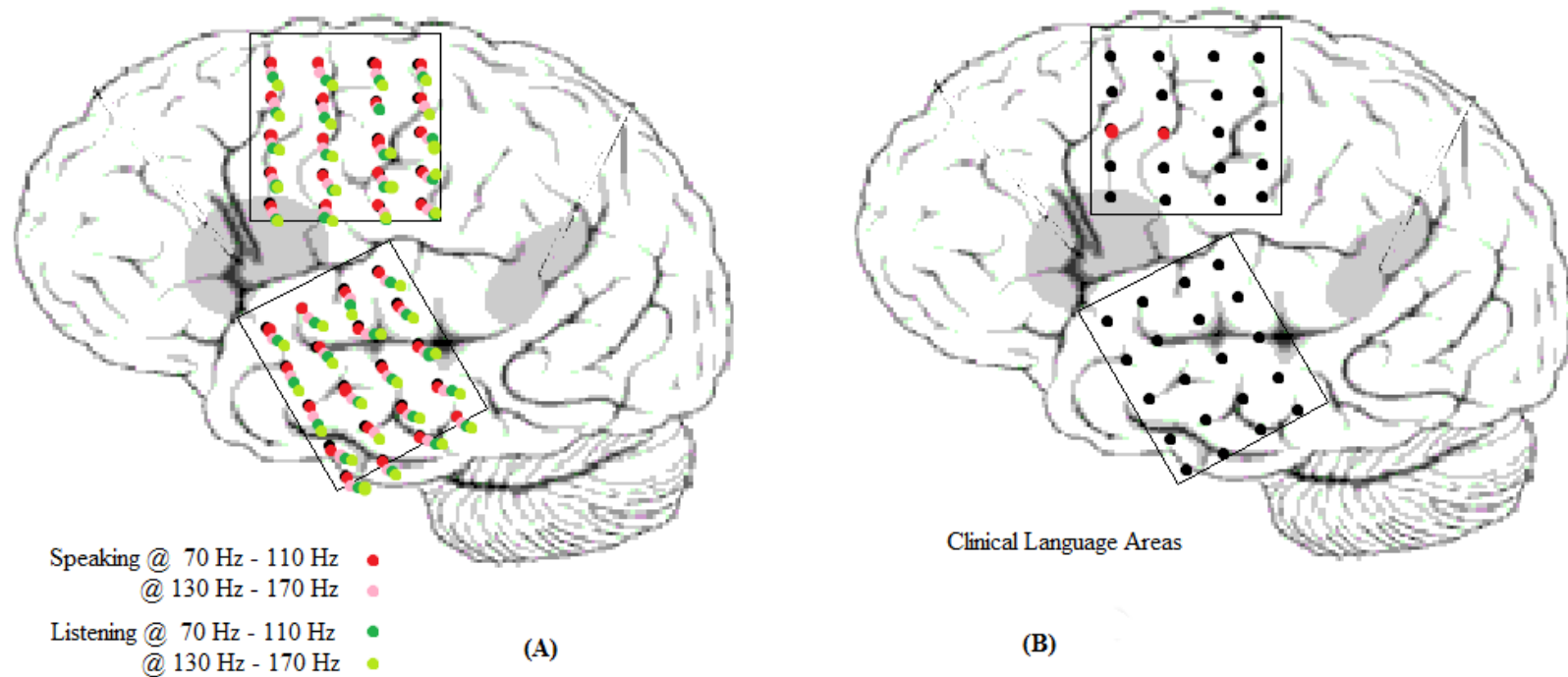


Figure 25: Two brains with electrodes found to be language-specific. The brain on the left illustrates statistically significant electrode activations during speaking and listening conditions for Patient 4 over the left temporal grid and estimated motor area (cross-referenced from CT images). The power of each language condition was estimated from the above frequencies and separated into similar segments. Speaking and listening were then compared to baseline.

Figure 26. Patient 4 Brain Sketch Ratios

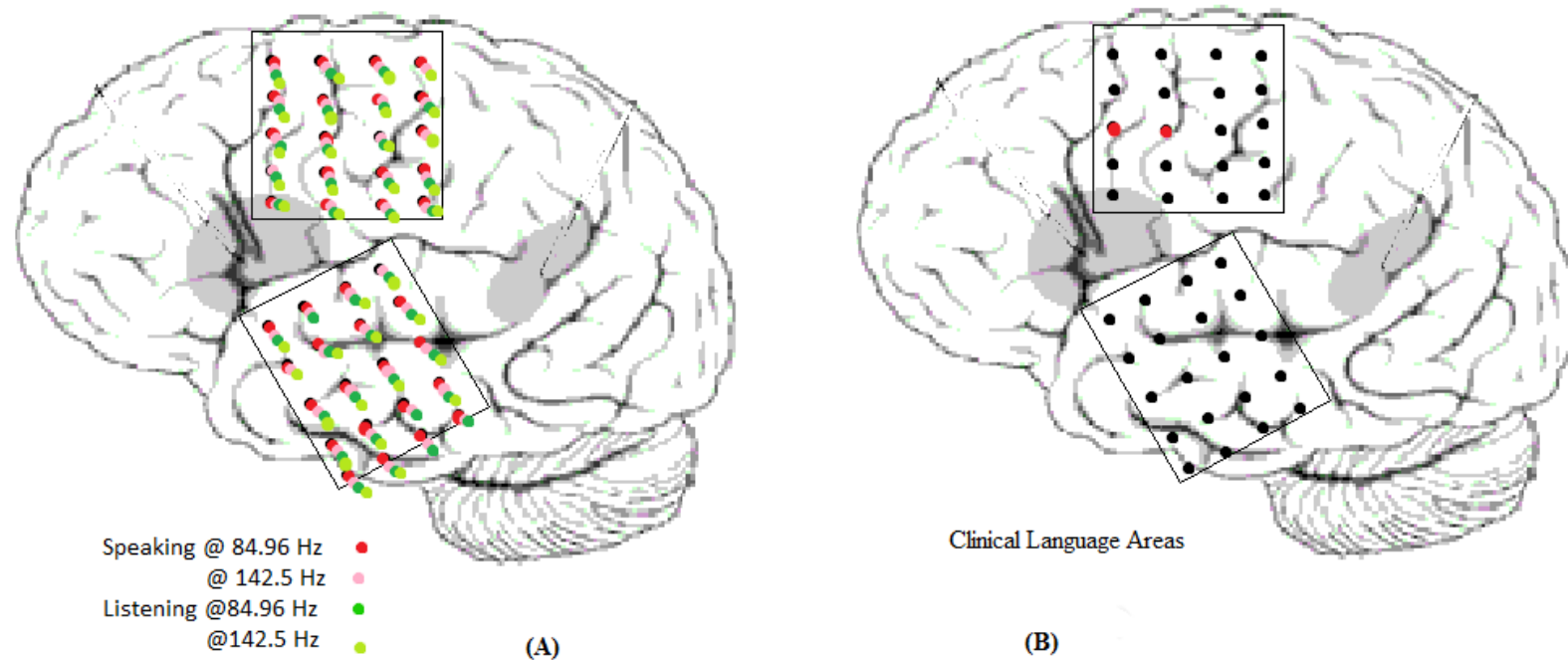


Figure 26: Two brains with electrodes found to be language-specific. The brain on the left illustrates statistically significant electrode activations during speaking and listening conditions for Patient 4 over the left temporal grid and estimated motor area (cross-referenced from CT images). The power of each language condition was estimated from the above specified frequencies and separated into similar segments; each condition was then divided by the averaged baseline. The power ratios of speaking and listening were compared to normalized baseline.

Figure 27. Patient 1 Brain Sketch Ratios (Frequency Ranges)

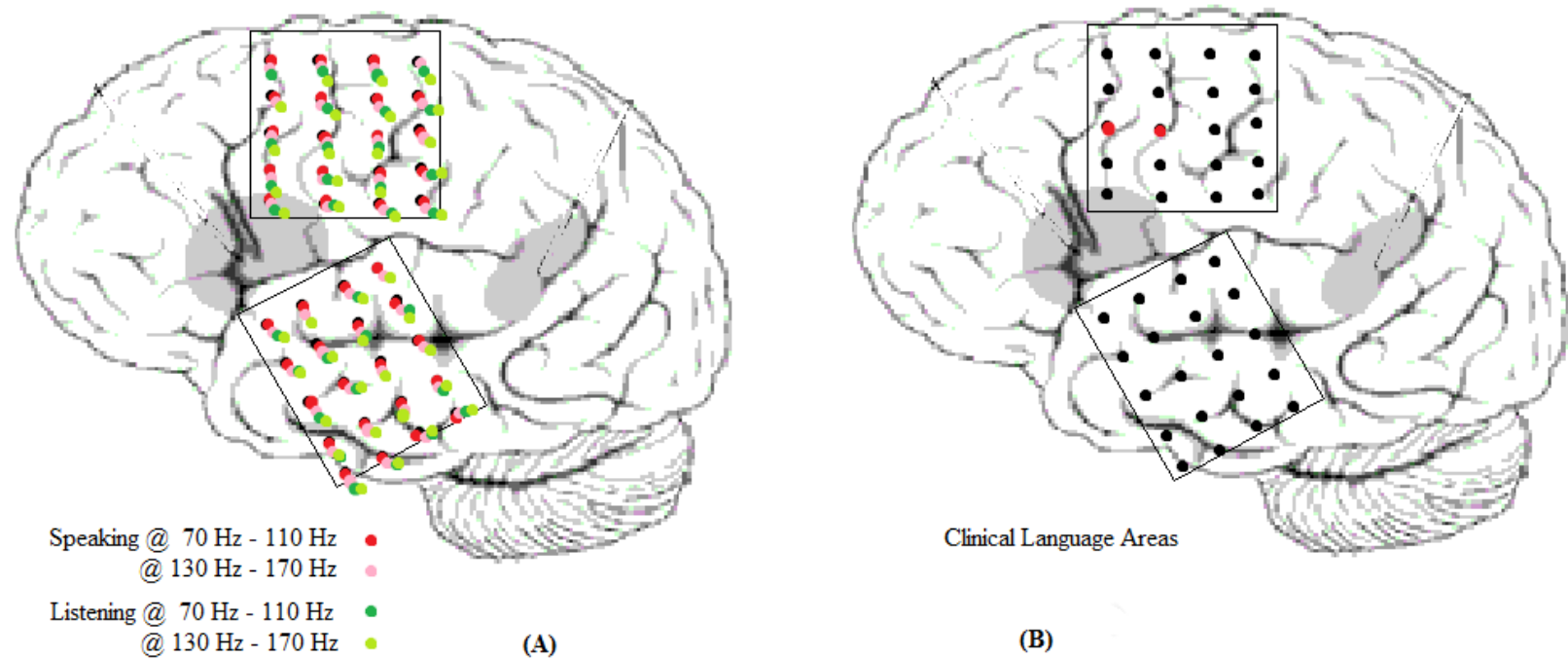


Figure 27: Two brains with electrodes found to be language-specific. The brain on the left illustrates statistically significant electrode activations during speaking and listening conditions for Patient 4 over the left temporal grid and estimated motor area (cross-referenced from CT images). The power of each language condition was estimated from the above specified frequencies and separated into similar segments; each condition was then divided by the averaged baseline. The power ratios of speaking and listening compared to normalized baseline.

Figure 28. Patient 4 Brain Sketch Combined Speech (Segments)

53

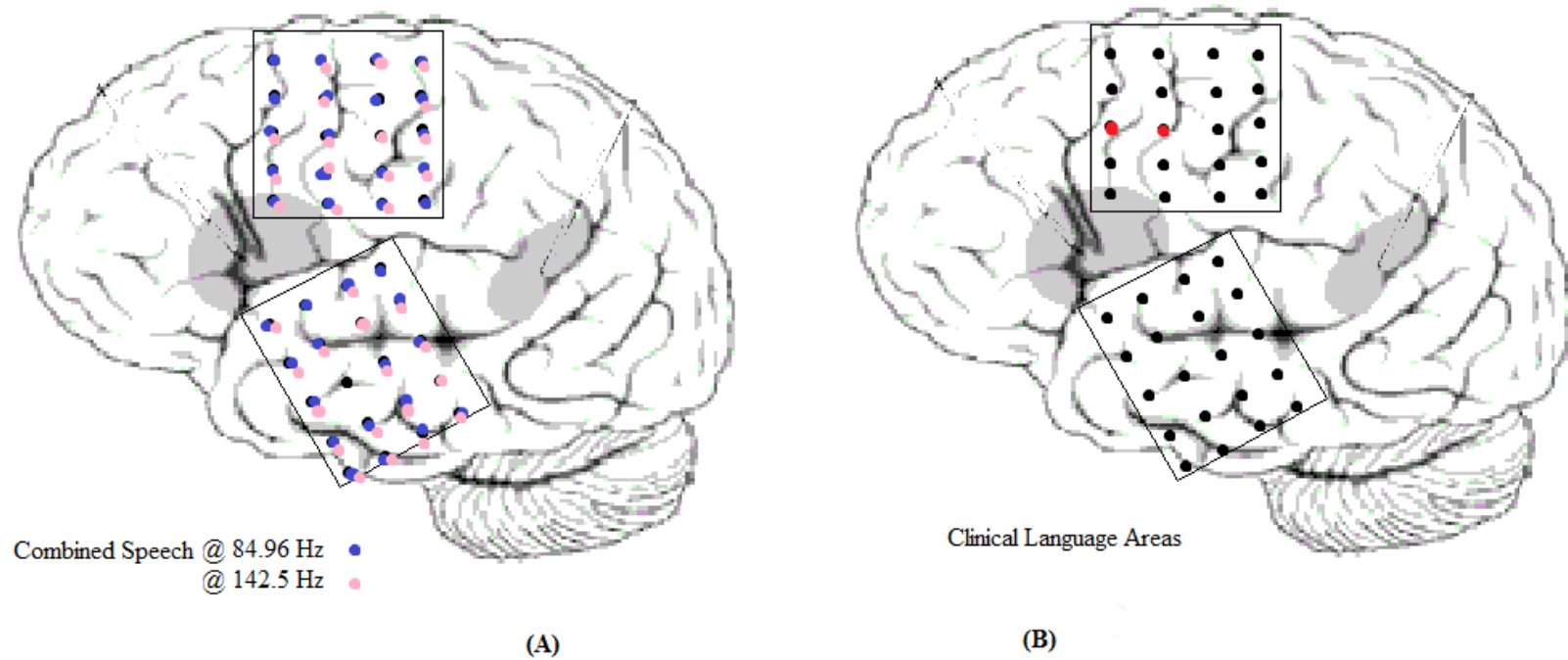


Figure 28: Two brains with electrodes found to be language-specific. The brain on the left illustrates statistically significant electrode activations during speaking and listening conditions for Patient 4 over the left temporal grid and estimated motor area (cross-referenced from CT images). The power of each language condition was estimated from the above frequencies and separated from baseline segments; the combined speech segments were then compared to baseline power.

Figure 29. Patient 4 Brain Sketch Combined Speech (Ratios)

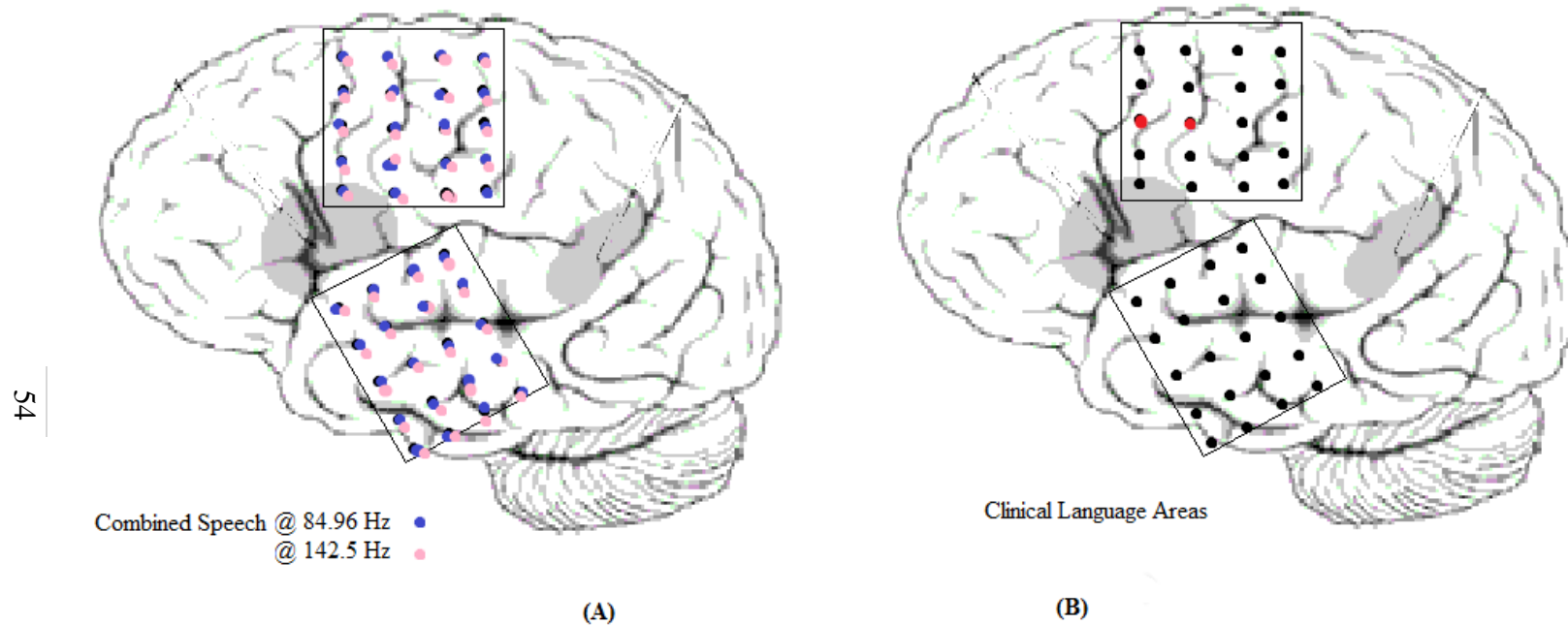


Figure 29: Two brains with electrodes found to be language-specific. The brain on the left illustrates statistically significant electrode activations during speaking and listening conditions for Patient 4 over the left temporal grid and estimated motor area (cross-referenced from CT images). The power of each language condition was estimated from the above specified frequencies and separated into similar segments; each condition was then divided by the averaged baseline. The speaking and listening power ratios were combined and compared to the baseline ratio.

Figure 30. Patient 5 Brain Sketch Listening

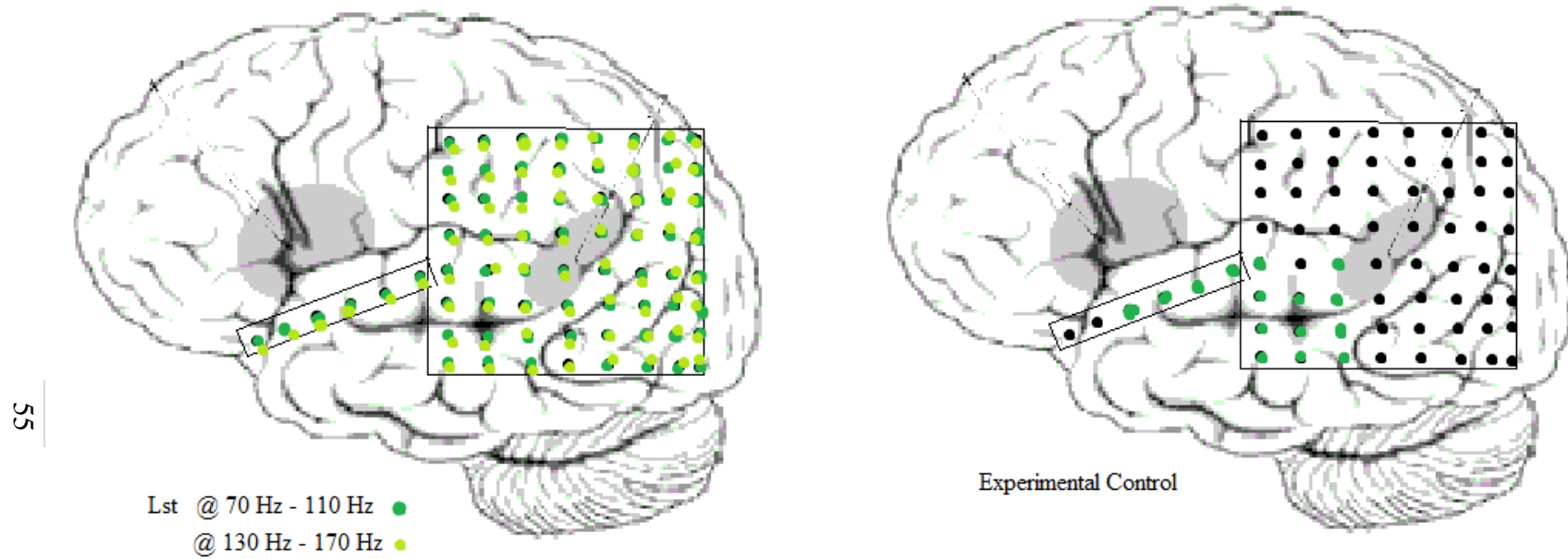


Figure 30: Two brains from Patient 5 with language-specific electrodes. The brain on the right illustrates activations found during an experiment in which the patient was listening to a computer generate words. The brain on the left yields statistically significant activations that were calculated from listening segments in a conversation. Power was calculated by a spectrogram. Notice only one electrode near inferior, posterior temporal lobe was similar to baseline during listening at 70-110 Hz.

Figure 31. Patient 5 Brain Sketch Speaking

56

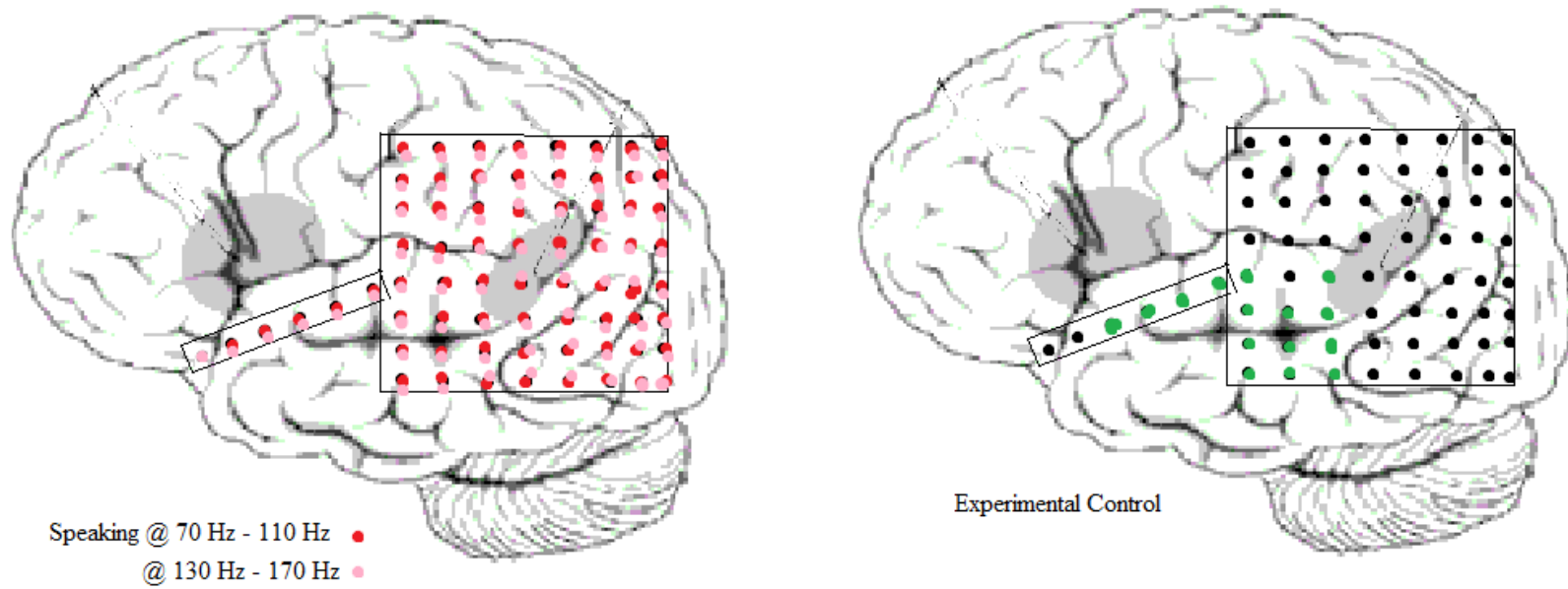


Figure 31: Two brains from Patient 5 with language-specific electrodes. The brain on the right illustrates activations found during an experiment in which the patient was listening to a computer generate words. The brain on the left yields statistically significant activations that were calculated from speaking segments in a conversation. Power was calculated by a spectrogram.

Figure 32. Patient 5 Brain Sketch Listening to Words

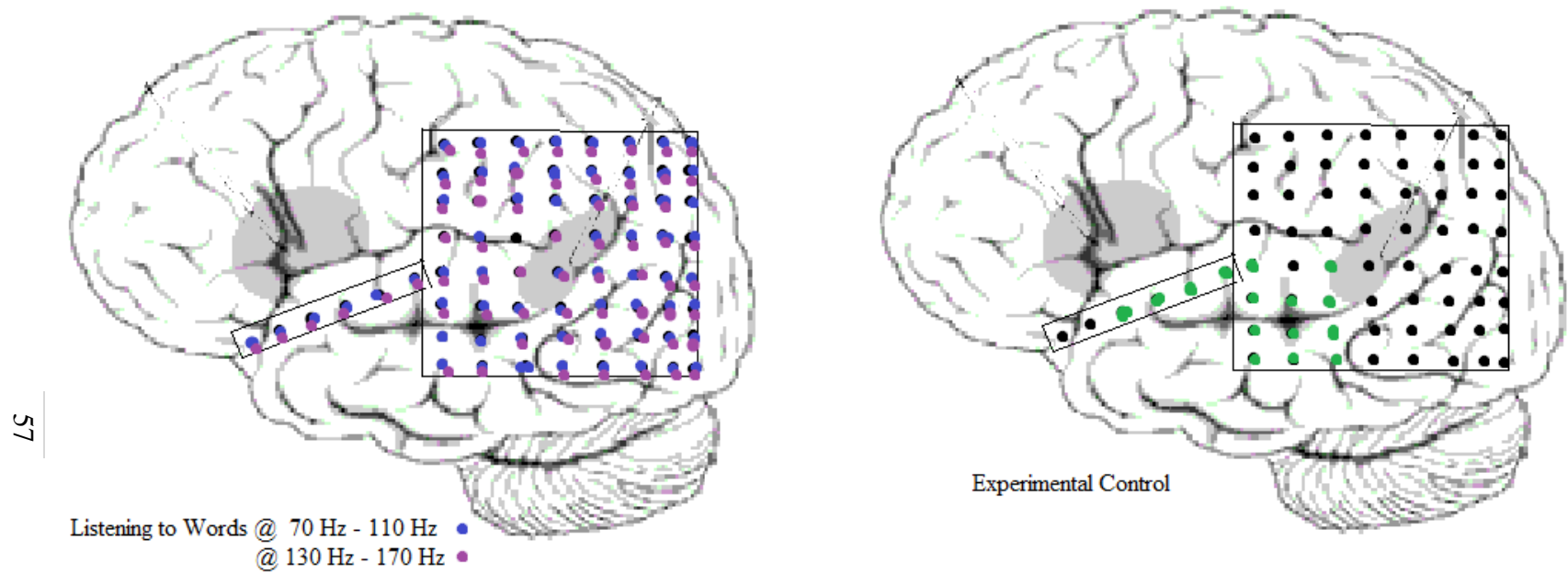


Figure 32: Two brains from Patient 5 with language-specific electrodes. The brain on the right illustrates activations found during an experiment in which the patient was listening to a computer generate words. The brain on the left yields statistically significant activations that were calculated from segments taken from which the experimental control was being conducted.

Figure 33. Patient 5 Brain Sketch Reading

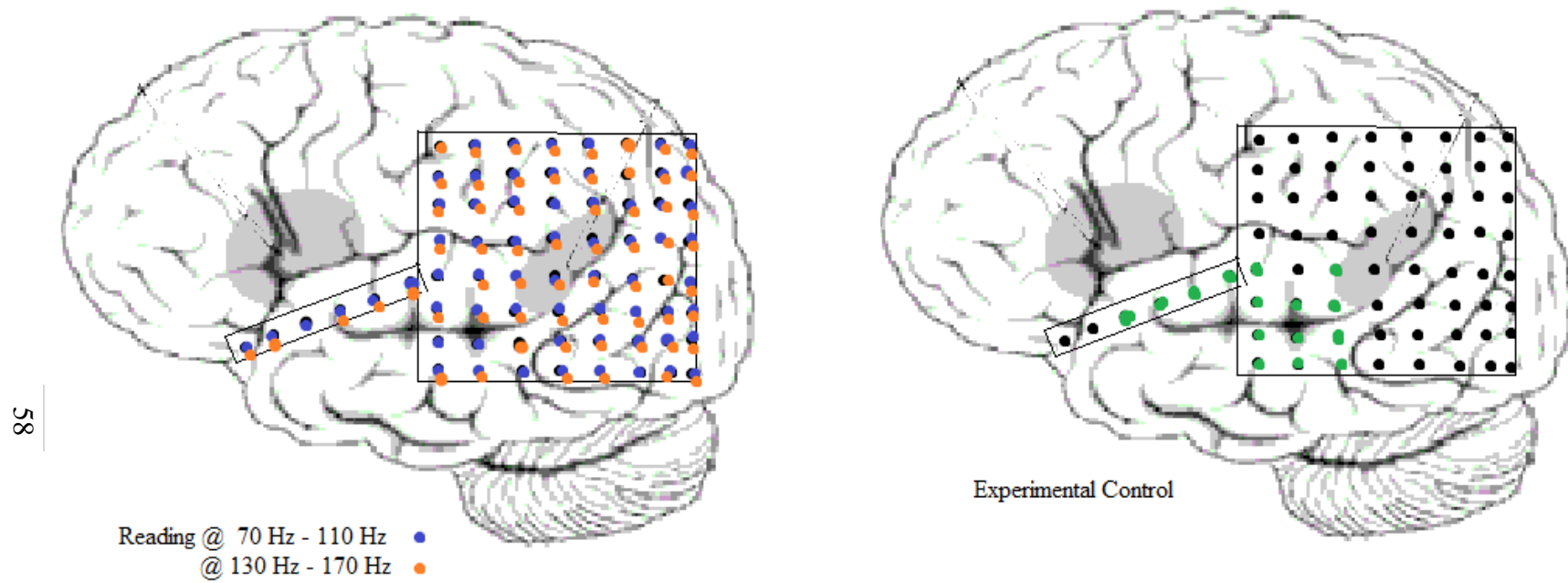


Figure 33: Two brains from Patient 5 with language-specific electrodes. The brain on the right illustrates activations found during an experiment in which the patient was listening to a computer generate words. The brain on the left yields statistically significant activations that were calculated from reading segments. Power was calculated by a spectrogram.

Figure 34. Patient 5 Brain Sketch Combined Speech

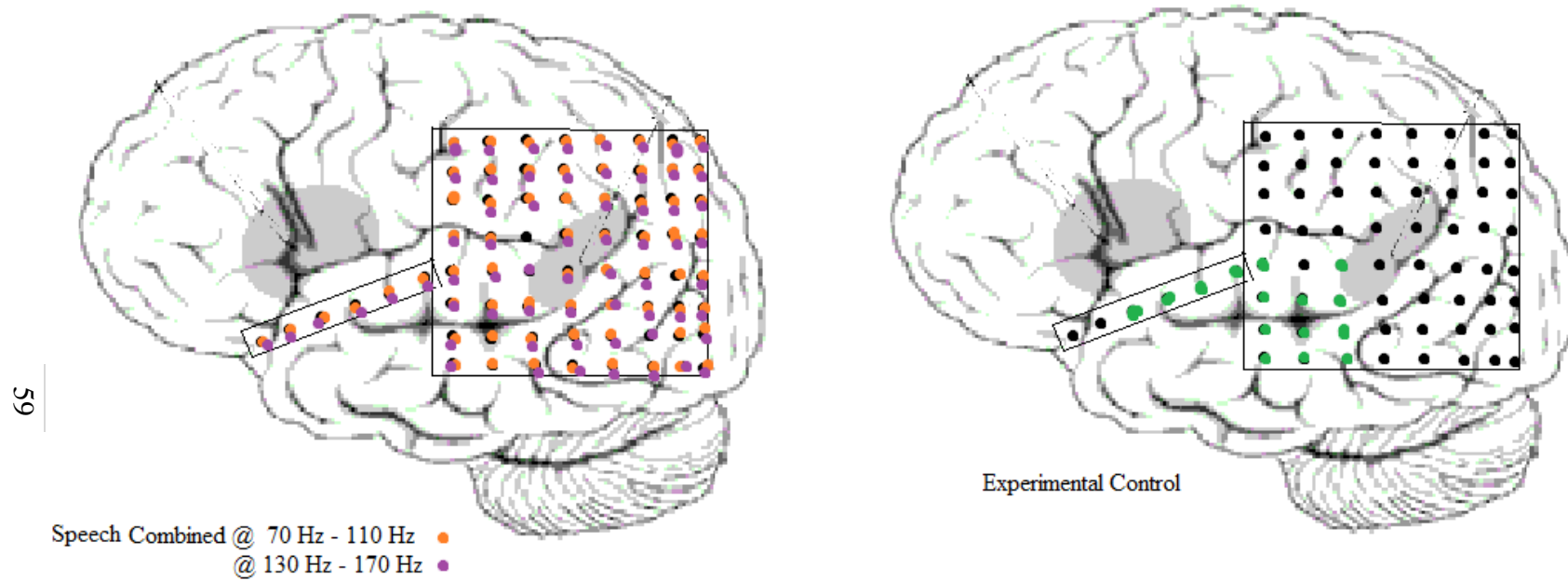


Figure 34: Two brains from Patient 5 with language-specific electrodes. The brain on the right illustrates activations found during an experiment in which the patient was listening to a computer generate words. The brain on the left yields statistically significant activations found when all speech conditions were combined. Power was calculated via spectrogram.

APPENDIX II
INSTITUTIONAL REVIEW BOARD APPROVAL FORM



November 8, 2012

Remy Wahnoun, PhD
Phoenix Children's Hospital
Neuroscience Department
1919 E Thomas Road
Phoenix, AZ 85016

RE: PCH IRB #: 12-104: Expressive and Receptive Language Mapping using EEG and ECoG (Expedited Review of New Study)

Dear Dr. Wahnoun:

I have reviewed your request for expedited approval of the new study listed above. Your study is eligible for expedited review under 21 CFR 56.110 and 45 CFR 46.110, category 5 where the research involves materials (data, documents, records, or specimens) that have been collected, or will be collected solely for non-research purposes (such as medical treatment or diagnosis).

A Waiver of Informed Consent has been granted under 45 CFR 46.116(d) (1-4).

A Waiver of HIPAA Authorization has been granted under 45 CFR 164.512(i)(1)(i)

The approval includes the following documents:

- IRB Paperwork (09/06/2012)
- Protocol and Data Collection Form for 12-104
- Request for Waiver of Informed Consent (09/04/2012)
- Request for Waiver of HIPAA Authorization (09/04/2012)

The study is next subject to continuing review on or before 11/07/2013, unless closed before that date. You may not continue the study beyond the expiration date noted above. You must apply for re-approval 45 days in advance of expiration to allow adequate time for IRB review.

As Principal Investigator you are responsible for assuring that:

- The approved protocol is followed and prior IRB approval is obtained for any changes (including changes in recruitment procedures, subject, population, location, protocol); and
- Any problems are reported promptly to the IRB (including adverse events and deviations from the approved protocol).

Approval period: 11/08/2012 - 11/07/2013

If you have any questions, please contact Cherie Putnam at 602-546-0141 or cputnam@phoenixchildrens.com.

Sincerely,

Mitchell Shub, MD
Co-Chair, PCH Institutional Review Board

cc: Jennapher Lingo VanGilder

1919 E. Thomas Rd. • Phoenix, AZ 85016 • (602) 933-1000 • (888) 908-5437 • www.phoenixchildrens.com